OSVZ-progenitors of human and ferret neocortex retain epithelial features and expand by integrin signaling

Wieland B Huttner

OSVZ-progenitors of human and ferret neocortex retain epithelial features and expand by integrin signaling

Simone A. Fietz[1*], Iva Kelava[1*], Johannes Vogt[2], Michaela Wilsch-Bräuninger[1], Denise Stenzel[1], Jennifer L. Fish[1], Denis Corbeil[4], Axel Riehn[3], Wolfgang Distler[3], Robert Nitsch[2] and Wieland B. Huttner[1§]

[1]Max Planck Institute of Molecular Cell Biology and Genetics, Pfotenhauerstrasse 108, D-01307 Dresden, Germany

[2]Institute of Cell Biology and Neurobiology, Center for Anatomy, Charité, Charitéplatz 1, D-10117 Berlin, Germany

[3]Klinik und Poliklinik für Frauenheilkunde und Geburtshilfe, Universitätsklinikum Carl Gustav Carus, Technische Universität Dresden, Fetscherstrasse 74, D-01307 Dresden, Germany

[4]BIOTEC, Technische Universität Dresden, Tatzberg 47-49, D-01307 Dresden, Germany

[*]Equal contribution to the ferret data shown in this study

[§]Corresponding author; huttner@mpi-cbg.de

Abstract

A major cause of expansion of the cerebral cortex during evolution is the increase in subventricular zone (SVZ) progenitors. Here we show that progenitors in the outer SVZ (OSVZ) of developing human neocortex, in contrast to rodent SVZ-progenitors which have limited proliferation potential, retain features of radial glia. While delaminating from apical adherens junctions, OSVZ-progenitors maintain a canonical epithelial property, a basal process contacting the basal lamina. OSVZ-progenitor divisions result in asymmetric inheritance of their basal process. Intriguingly, OSVZ-progenitors are also found in the ferret, a gyrencephalic non-primate. Functional disruption of integrins, expressed on the basal process of ferret OSVZ-progenitors, markedly decreases their population size, but not that of other, process-lacking, SVZ-progenitors, in slice culture of ferret neocortex. Our findings suggest that maintenance of a key epithelial property allows integrin-mediated, repeated asymmetric divisions of OSVZ-progenitors, providing a basis for neocortical expansion.

Introduction

Cortical expansion is a hallmark of mammalian brain evolution. A major underlying cause is the increase in the population size of neural progenitors and in the number of neurogenic divisions they undergo during cortical development[1-5]. Two principal classes of neural progenitors exist in the developing cortex[6,7]. The first comprises neuroepithelial cells and the radial glial cells (RGCs) they transform into with the onset of neurogenesis. These progenitors, which exhibit characteristics of neural stem cells, show apical-basal cell polarity and span the cortical wall from the basal lamina (pia) to the ventricular (apical) surface, with their cell bodies occupying the apical-most layer of the cortical wall, the ventricular zone (VZ). These VZ-progenitors are connected by adherens junctions at the apical-most end of their lateral plasma membrane, and their primary cilium protrudes from the apical plasma membrane into the ventricular lumen. The resulting apical localization of their centrosomes results in their mitosis occurring at the ventricular surface, which is why these progenitors have also been collectively referred to as apical progenitors (APs). Their mitosis is followed by interkinetic nuclear migration (INM), that is, the apical-to-basal movement of their nuclei in G1 for S phase at an abventricular location and the basal-to-apical movement of their nuclei in G2 for the next mitosis. INM is the reason for the pseudostratified appearance of the VZ[4,7].

The second class of neural progenitors in the developing cortex, which so far have been studied mostly in rodents, are cells that are born from APs in the VZ but that delaminate from the apical belt of adherens junctions and migrate in the basal direction to form, and to typically divide in, a second, more basal, progenitor layer, the SVZ[1,6]. In rodents, these progenitors retract their apical and basal processes during their cell cycle, have lost apical-basal polarity by M phase, and in most instances divide only once to generate two neurons[1,6,8].

Given their basal location and intermediate nature in the lineage from APs to neurons, these progenitors have been referred to as basal[6] or intermediate[1] progenitors.

APs expand by symmetric proliferative divisions. This determines the size of the primary progenitor population, and hence of the number of radial units[5]. Spatial accommodation of the increasing number of APs is achieved by them becoming very elongated, which in turn increases the degree of pseudostratification of the VZ[4]. In addition, this proliferation results in the lateral expansion of the VZ[5].

It is, however, the expansion of the SVZ that constitutes the most striking difference between mammals showing various degrees of cortical expansion[1,3,4]. As the proliferative potential of rodent basal progenitors (BPs) is very limited[1,6], in contrast to that of APs, the question arises whether this could, perhaps, be due to differences in the cell biology of these progenitors. A corollary of this consideration is whether SVZ-progenitors in species developing a gyrencephalic cortex, that is, a cortex with a laterally expanded, folded pial surface, exhibit cell biological features distinct from their counterparts in species with a lissencephalic, smooth cortical surface such as rodents.

A key observation in this regard has been the description of a unique germinal layer in the monkey, referred to as OSVZ[9]. A characteristic morphological feature of the monkey OSVZ, in contrast to the rodent SVZ, is its radial appearance, which has led to the suggestion that the OSVZ may harbor cell bodies of RGCs[9]. Extending this to the cell biological level, we previously hypothesized that OSVZ-progenitors maintain certain epithelial features, and that it is this maintenance which endows them with the capacity for self-renewal and which is required for OSVZ expansion (epithelial progenitor hypothesis)[4]. In the present study, we have investigated this hypothesis. We find that OSVZ-progenitors exist not only in primates, notably human, but also in a non-primate species developing a gyrencephalic cortex, the ferret, with the branch point in the phylogenetic tree for these two species dating back 97

million years[10]. OSVZ-progenitors indeed exhibit a canonical epithelial feature, that is, the contact with the basal lamina throughout their cell cycle via retention of a basal process. Moreover, we show that integrin function is required to ensure the full population size of these basal process-bearing OSVZ-progenitors.

Results

Human OSVZ-progenitors exhibit characteristics of RGCs

To define the molecular nature of human OSVZ-progenitors, we first considered the abventricular location of their nuclei and therefore investigated the expression of Tbr2, a transcription factor characteristically expressed in SVZ-progenitors in rodents[11,12]. In line with observations by others[13], Tbr2 immunoreactivity was much more pronounced in the SVZ than VZ of 10-week-old human neocortex (**Fig. 1e**). Interestingly, as the human SVZ developed further and the distinct ISVZ and OSVZ emerged during 12-16 weeks post-conception (w.p.c.), Tbr2 was more prominent in the human ISVZ than OSVZ (**Fig. 1g**, **i**, **k**). This suggests that human ISVZ-progenitors are more related to rodent SVZ-progenitors than is the case for human OSVZ-progenitors, and raised the possibility that OSVZ-progenitors might exhibit features not typically observed for rodent SVZ-progenitors.

To explore this further, we investigated the expression of Pax6, a transcription factor characteristically expressed in rodent VZ-progenitors but down-regulated in rodent SVZ-progenitors[4,11,12,14]. At 10 w.p.c., similar to observations in rodents, Pax6 immunoreactivity was abundant in the human VZ but sparse in the SVZ (**Fig. 1d**) and strikingly different from the expression of Tbr2 between these two germinal layers (**Fig. 1e**). Remarkably, concomitant with the emergence of the human OSVZ during 12-16 w.p.c., Pax6-positive nuclei progressively appeared in the OSVZ, seemingly at the expense of the VZ which became thinner (**Fig. 1f**, **h**, **j**). These data confirm and extend previous reports on the expression of Pax6 in the primate OSVZ[4,13,15] and suggest a close relationship between OSVZ- and VZ-progenitors.

To corroborate the progenitor nature of the Pax6- and the Tbr2-positive cells in the human VZ, SVZ and – when discernible – ISVZ and OSVZ, and to obtain quantitative data,

we confined our analysis to mitotic cells as revealed by phosphohistone H3 (PH3) immunostaining. At 10 w.p.c., consistent with previous observations[16], the location of mitotic figures was similar to that in rodents at early stages of neurogenesis, with the vast majority being found at the ventricular surface, whereas at later stages the relative increase in mitotic figures in the human SVZ in comparison to the mouse SVZ became evident (data not shown). At any of the developmental stages examined, >95% of progenitors in the VZ showed Pax6 expression (**Fig. 1a**), while only <5% of them were Tbr2-positive (**Fig. 1a**). Pax6 expression was also observed for the vast majority (>80%) of progenitors in the human SVZ (**Fig. 1b**). Separate analysis of the ISVZ and OSVZ at 16 w.p.c. revealed that only about half of the progenitors in the ISVZ were Pax6-positive, whereas ≈90% of progenitors in the OSVZ were Pax6-positive (**Fig. 1c**). The proportion of Tbr2-positive progenitors in the human SVZ decreased from >80% at 10 w.p.c. to <60% at 16 w.p.c. (**Fig. 1b**). Separate analysis of the ISVZ and OSVZ at 16 w.p.c. revealed that, conversely to Pax6, almost all progenitors in the ISVZ, but less than half of the progenitors in the OSVZ, were Tbr2-positive (**Fig. 1c**). Together, these data suggest the existence of at least two progenitor subpopulations in the human SVZ, ISVZ-progenitors which express Tbr2 but down-regulate Pax6 expression and hence resemble rodent BPs, and OSVZ-progenitors which do not generally sustain Tbr2 expression but like VZ-progenitors maintain Pax6 expression and thus have no counterpart in the rodent SVZ. (For the Pax6/Tbr2 double-positive progenitors in the human SVZ, the existence of which is implicit from our quantitations (**Fig. 1b**, **c**), see below.)

These observations prompted us to explore the possible presence, in human OSVZ-progenitors, of other, cytoplasmic, markers characteristically expressed in VZ-progenitors. Specifically, we examined the presence of nestin, expressed in neuroepithelial cells as well as RGCs[17], of BLBP and GLAST, two proteins expressed in VZ-progenitors after their transformation into RGCs[17], and of GFAP, expressed in primate[18], but not early rodent[19],

RGCs. All four proteins were readily detected not only in the human VZ but also in the human OSVZ at 11-16 w.p.c. (**Fig. 2**). Importantly, in either germinal layer, overt immunostaining for these proteins, notably nestin (**Fig. 2a**), was not only present in traversing radial fibers, as was the case for the ISVZ, but also in the cell body cytoplasm (**Fig. 2a**, **c**, **e**–**g**, arrowheads), indicative of expression in VZ- and OSVZ-progenitors. The latter conclusion was corroborated for SVZ-progenitors by double immunofluorescence for nestin and PH3 (**Fig. 2a**). These data show that human OSVZ-progenitors, in contrast to rodent BPs, maintain expression of cytoplasmic markers characteristic of VZ-progenitors and hence are more closely related to the latter than is the case for rodent BPs.

Human OSVZ-progenitors retain a basal process in M-phase

A remarkable cell biological feature of rodent VZ-progenitors is the retention of their basal processes through M-phase[20-22], whereas rodent BPs in M-phase lack processes of any significant length[8]. Given the close relationship of human OSVZ-progenitors to VZ-progenitors with regard to molecular marker expression, and the presence of a basal process in monkey OSVZ-progenitors in interphase[23], we investigated whether human OSVZ-progenitors exhibit basal processes and retain them through M-phase. DiI labeling from the pial side of 13-w.p.c. human cortical sections revealed the presence of processes that extended from the pial surface to cell bodies residing in the OSVZ and VZ (**Fig. 3a**). Immunostaining for phosphorylated vimentin, a mitotic marker[24], demonstrated that not only VZ-progenitors undergoing mitosis at the ventricular surface (**Fig. 3b**) but also progenitors undergoing mitosis in the SVZ (**Fig. 3c**) extended a basal process in M-phase (**Fig. 3d**). The latter basal process-bearing mitotic cells were indeed OSVZ (rather than ISVZ) progenitors because virtually all of them were Pax6-positive (**Fig. 3e**, **g**) and <5% were Tbr2-positive (**Fig. 3f**, **g**).

The latter data also suggest that the Pax6/Tbr2 double-positive progenitors in the human SVZ (**Fig. 1b**) belonged to the ISVZ-progenitor subpopulation.

Neither the DiI labeling from the pial surface nor the phosphovimentin immunostaining provided evidence for the presence of an apical process extending from OSVZ-progenitors at M-phase (**Fig. 3c**, **e**, **f).** We next investigated whether OSVZ-progenitors expressed markers characteristically observed at the apical domain of VZ-progenitors, i.e. prominin-1 (CD133), an apical plasma membrane protein[25], Par3, associated with their apical cell cortex[26-28], and ZO-1, associated with apical adherens junctions[29]. All three apical domain markers were highly concentrated at, or near, the ventricular surface of the human 13-w.p.c. cortical wall, as previously observed for the cortical wall of rodents, but not in the SVZ (**Suppl. Fig. 1a**–**e**). In-situ-hybridization for prominin-1 mRNA showed that human OSVZ-progenitors, in contrast to VZ-progenitors, lacked prominin-1 expression (**Suppl. Fig. 2**). Together, these data indicate that human OSVZ-progenitors exhibit some, but not all, of the epithelial features of VZ-progenitors. They are polarized, extending a basal process to the basal lamina that is retained through M-phase, but apparently lack an apical process at M-phase and down-regulate apical domain marker expression.

Perinuclear centrosomes in human OSVZ-progenitors

We next analyzed the distribution of centrosomes in the human VZ, ISVZ and OSVZ. Immunofluorescence of 17-w.p.c. human neocortex for the centrosome marker γ-tubulin showed abundant staining at the ventricular surface, with the remainder of the VZ containing only relatively few centrosomes (**Fig. 4b**, **c** VZ), as observed previously for rodents[30]. Compared to the non-surface region of the VZ, centrosome abundance was increased in the human ISVZ and OSVZ and appeared to match that of the nuclei in these zones (**Fig. 4c** ISVZ and OSVZ). Quantification of centrosomes at the ventricular surface relative to apical endfeet

by EM (**Fig. 4f**, **g**) revealed a 1:1 ratio (**Table 1**). Moreover, we observed at least one centrosome per OSVZ-progenitor nucleus in interphase (**Table 1**), which was located in its immediate vicinity (**Fig. 4d**, **e**). Together, these data are consistent with the notion that essentially all apical centrosomes belonged to VZ- progenitors only (rather than both VZ- and OSVZ-progenitors) and that OSVZ-progenitors lack an apical process extending all the way to the ventricular surface, and imply that OSVZ-progenitor nuclei can proceed to mitosis at their interphase location.

Human OSVZ-progenitors show random cleavage orientation

Given that mouse BPs lack apical-basal polarity in M-phase and show a near-random cleavage plane orientation[8], the finding that human OSVZ-progenitors in M-phase exhibit basal polarity (**Fig. 3a**–**g**) raised the question whether they show a random cleavage plane orientation or, like the basal process-bearing VZ-progenitors, an orientation predominantly parallel to their radial axis. Analysis of >100 mitotic human OSVZ-progenitors revealed a near-random orientation of their mitotic spindle as deduced from the position of the sister chromatids at anaphase (**Fig. 5a**, **b**). The same result was obtained when Pax6-positive mitoses in the SVZ were analyzed for cleavage orientation (**Fig. 5c**). This was in striking contrast to mitotic human VZ-progenitors, the anaphase spindles of which showed a clear preference for an orientation largely parallel to the ventricular surface (**Fig. 5a**, **b**), predicting a cleavage plane largely parallel to the radial, apical-basal axis of the cells, as has been known to be the case for the vast majority of rodent VZ-progenitor[4,6,27,31].

Interestingly, analysis of >150 mitotic human ISVZ-progenitors revealed a predicted cleavage plane orientation distinct from both VZ and OSVZ-progenitors. Although there was a substantial (≥25%) contribution by the "vertical" (60-90°) and the "oblique" (30-60°) category of cleavage plane orientations, almost half of them fell into the "horizontal" (0-30°)

category (**Fig. 5a**, **b**). The same result was obtained when Tbr2-positive mitoses in the SVZ were analyzed for cleavage orientation (**Fig. 5c**). This non-random cleavage plane orientation of ISVZ-progenitors is reminiscent of that of rat[22] (but not mouse[8]) basal/intermediate progenitors.

The random cleavage plane orientation of OSVZ-progenitors implies that the inheritance of their basal process and basally polarized cell fate determinants by the daughter cells will be asymmetric. Indeed, phosphovimentin immunofluorescence of dividing human OSVZ-progenitors showed inheritance of the basal process by one of the nascent daughter cells (**Fig. 5d**–**g**). Interestingly, we noticed that occasionally the other daughter cell, still connected to the former via the midbody, extended a process in the opposite, apical direction (**Fig. 5g**).

OSVZ-progenitors exist in ferret neocortex

Given the molecular and cellular features of human OSVZ-progenitors described above, which render these cells distinct from rodent BPs, it was of interest to explore whether OSVZ-progenitors are specific to primates, as previously discussed[9], or can also be found in other brains exhibiting a gyrencephalic cerebral cortex. To investigate this possibility, we turned to the ferret, a gyrencephalic non-primate. Specifically, we chose ferret cortex of embryonic day (E) 32, which in terms of cortical development corresponds approximately to human 10 w.p.c., ferret E39 cortex corresponding approximately to human 14 w.p.c., and ferret cortex of postnatal day (P) 10, i.e. a late stage of neurogenesis at which the ferret cortex shows overt gyrencephaly[32,33]. These stages of ferret cortical development were subjected to the same type of analyses as performed for human fetal neocortex.

Regarding Pax6 and Tbr2 expression, the ferret SVZ was found to be very similar to the human SVZ and distinct from the rodent SVZ, with Pax6-positive nuclei progressively

appearing in the SVZ at the expense of the VZ (**Fig. 1n**, **p**, **r**), and with Tbr2-positive nuclei being concentrated in the region of the embryonic SVZ that abutted on the VZ (**Fig. 1o**, **q**, **s**). As in the developing human neocortex, the mitotic cells in the ferret VZ were Pax6-positive (**Fig. 1l**) and largely Tbr2-negative (**Fig. 1l**), and the mitotic cells in the ferret SVZ were almost all Pax6-positive (**Fig. 1m**), with Tbr2 expression decreasing from ≈80% to ≈40% during cortical development (**Fig. 1m**).

Similarly, the cytoplasmic markers of VZ-progenitors and specifically RGCs in rodents, nestin, GLAST and BLBP, were all found in the cell body not only of VZ-progenitors, but also SVZ-progenitors in the E39 ferret neocortex (**Suppl. Fig. 3**), the main difference to the fetal human neocortex being the lack of GFAP expression in the embryonic (but not postnatal) ferret neocortex (data not shown), as is the case for the early embryonic rodent neocortex[19]. Together, these data demonstrate that a major subpopulation of ferret SVZ-progenitors resemble human OSVZ-progenitors with regard to the expression of molecular markers that in rodents are characteristic of APs rather than BPs. Our conclusion that these ferret SVZ-progenitors are of the OSVZ-type and distinct from rodent BPs was further supported by Nissl staining which revealed cytoarchitectonically distinct zones within the ferret SVZ, consistent with the existence of an ISVZ and OSVZ, and a radial appearance of the progenitors in the outer region of the E39 ferret SVZ (data not shown).

Ferret OSVZ-progenitors retain a basal process in M-phase

We next determined whether ferret OSVZ-progenitors extend basal processes and retain them through M-phase. Indeed, DiI labeling from the pial side of E39 cortical sections revealed that progenitors in the ferret SVZ, identifiable as cycling cells by Ki67 immunostaining (**Fig. 3i**), extended basal processes all the way to the pial surface and in several of these cases also showed an apical process directed towards, but not reaching, the

ventricular surface (**Fig. 3h**). Moreover, ferret OSVZ-progenitors, like VZ-progenitors (**Fig. 3j**), retained their basal processes through M-phase as indicated by phosphovimentin immunostaining (**Fig. 3k**, **l**). Virtually all of these mitotic basal process-bearing ferret OSVZ-progenitors were Pax6-positive (**Fig. 3m**, **o**) and Tbr2-negative (**Fig. 3n**, **o**), despite the presence of Tbr2-positive mitotic cell bodies in the ferret SVZ (**Fig. 1o**, **q**, **s**). However, in contrast to ferret OSVZ-progenitors in interphase (**Fig. 3h**, **i**), we did not observe apical processes of any significant length in mitotic ferret OSVZ-progenitors (**Fig. 3k**, **m**, **n**). Accordingly, apical domain marker expression (Par3, aPKC, ZO-1) was prominent in ferret VZ-, but not OSVZ-, progenitors (**Suppl. Fig. 1f**–**k**), as observed for fetal human neocortex (**Suppl. Fig. 1a**–**e**).

We conclude that the ferret SVZ, like the human SVZ, contains at least two progenitor populations. One comprises progenitors that resemble rodent BPs in that they express Tbr2 and lack processes of any significant length in mitosis, and hence appear to be unpolarized when undergoing cell division. These progenitors are found mostly in the region of the SVZ that abuts on the VZ, consistent with the existence of an ISVZ in the ferret. The other ferret SVZ-progenitor population comprises cells with features distinct from rodent BPs, including maintenance of Pax6 and cytoplasmic VZ-progenitor marker expression, and retention of a basal process through mitosis which implies basal polarity in M-phase. These progenitors are found throughout the ferret SVZ, being apparently sparser in the ISVZ, and by all criteria examined resemble human OSVZ-progenitors.

We next analyzed the cleavage plane orientation of E39 ferret progenitors. This revealed that the predicted cleavage planes of mitotic SVZ-progenitors were distributed over all three categories of orientation, with a slight preference for a horizontal orientation (**Fig. 5h**). Separate analyses of Pax6-positive and Tbr2-positive ferret SVZ mitoses (**Fig. 5i**) showed that the preference for a horizontal orientation was characteristic of the latter, with a

near-random orientation of the former. This was in contrast to mitotic VZ-progenitors, ≈90% of which showed a predicted cleavage plane orientation largely parallel to the radial, apical-basal axis of the cells (**Fig. 5h**). Moreover, consistent with the data on cleavage plane orientation, the basal processes of mitotic ferret OSVZ-progenitors were found to be inherited by only one of the daughter cells (**Fig. 5j**, **k**), indicative of asymmetric division, as was found to be the case for human OSVZ-progenitors (**Fig. 5d**–**g**).

OSVZ-progenitors depend on integrin function

The finding that the ferret SVZ contains OSVZ-progenitors, which so far have been reported only for primates[9], offered an experimental system to explore the significance of their basal process retention and basal lamina contact. An intriguing target of investigation in this regard are integrin receptors[34-37]. Integrin function can be potently blocked by disintegrins, snake venoms which prevent ligand binding to certain, RGD-sensitive, integrins[38]. Integrins, notably integrin $\alpha_5\beta_1$ and α_v, have previously been shown to be expressed on nestin-positive cortical progenitors, i.e. RGCs, in rodents[39,40]. We therefore investigated the effects of echistatin, a disintegrin with high affinity for $\alpha_5\beta_1$ and $\alpha_v\beta_3$ integrins[41], on SVZ-progenitors in organotypic slice culture of E40 ferret telencephalon.

Exposure of E40 ferret neocortex for up to 4 days to 4 μM echistatin, a concentration previously used for neural stem cell cultures in vitro[42], significantly reduced the population size of cycling progenitors, identified by Ki67 immunofluorescence (**Fig. 6**, green, compare **b** and **d** with **a** and **c**, respectively; **Fig. 6f**). This reduction was detected after 2-4 days of culture and was observed in both the VZ and SVZ, but the magnitude of the reduction was greater for the SVZ (maximally 83%, **Fig. 6l**) than for the sum of VZ plus SVZ (maximally 48%, **Fig. 6f**). In light of the observations that the mitotic basal process-bearing ferret SVZ-progenitors are Pax6-positive and Tbr2-negative whereas mitotic Tbr2-positive SVZ-

progenitors only very rarely, if at all, show a basal process (**Fig. 3m**–**o**), we used these markers to investigate whether, perhaps, the reduction in Ki67-positive cells selectively affected the Pax6-positive/Tbr2-negative, but not the Tbr2-positive, progenitor subpopulation.

Remarkably, the Tbr2-positive subpopulation of Ki67-positive progenitors, analyzed in the sum of VZ plus SVZ (**Fig. 6g**) as well as in the SVZ alone (**Fig. 6m**), was largely unaffected by echistatin treatment, whereas the Tbr2-negative subpopulation was reduced to more than half (**Fig. 6h**, **n**). Consistent with this, the Pax6-positive subpopulation of Ki67-positive progenitors was markedly reduced by echistatin treatment (**Fig. 6i**), whereas the Pax6-negative subpopulation was essentially unaffected (**Fig. 6j**). Again, the magnitude of the reduction in the Pax6-positive and Tbr2-negative subpopulation was greater for the SVZ (maximally 87% for Pax6, **Fig. 6k**) than for the sum of VZ plus SVZ (maximally 73% for Pax6, **Fig. 6i**). Taken together, these data indicate that interference with integrin function by exposure to disintegrins selectively reduces the population size of those ferret SVZ-progenitors that characteristically retain a basal process throughout their cell cycle.

To corroborate these observations, we used a different form of interference, the addition of blocking antibodies targeting specific integrins. Addition of 25 μg/ml of antibody against $\alpha_v\beta_3$ integrin to organotypic slice cultures of E40 ferret telencephalon for four days markedly reduced the numbers of the total Ki67-positive, the Pax6/Ki67 double-positive and the Tbr2-negative/Ki67-positive progenitors in the SVZ, without affecting the Pax6-negative/Ki67-positive SVZ-progenitors (**Fig. 6e**). We conclude that disruption of $\alpha_v\beta_3$ integrin function by blocking antibody reduces the population size of ferret OSVZ-progenitors.

Beta-3-integrins on the basal process of OSVZ-progenitors

If the reduction in the Pax6-positive/Tbr2-negative subpopulation of ferret SVZ-progenitors, i.e. OSVZ-progenitors, upon disintegrin treatment or addition of blocking antibody reflected basal process-mediated integrin function, one would expect the presence of the relevant integrin(s) on the basal process of ferret SVZ-progenitors. We investigated this by immunostaining of mitotic basal process-bearing E39 ferret SVZ-progenitors for beta-3-integrin. Indeed, beta-3-integrin was detected in these processes, being concentrated in distal varicosities (**Fig. 7a**, **b**). Consistent with the close relationship between OSVZ- and VZ-progenitors, we also observed beta-3-integrin–positive varicosities on the basal process of VZ-progenitors (**Fig. 7c**, **d**). We conclude that retention of the basal process may endow OSVZ-progenitors with the capacity for basal process-triggered integrin signaling, which is required for ensuring the full population size of these progenitors.

Discussion

Our study identifies a specific cell biological feature of neural progenitors that appears to be linked to a hallmark of neocortex expansion, the increase in the SVZ. Specifically, OSVZ-progenitors in the developing, eventually gyrencephalic cortex of human and ferret differ from the SVZ-progenitors of the lissencephalic rodent cortex in that they retain, throughout the cell cycle, a basal process contacting the basal lamina. This retention has significant implications for the issue of cell polarity of SVZ-progenitors and whether their divisions are cell biologically symmetric or asymmetric, which in turn may influence their capacity for self-renewal and may be of major importance for the magnitude of their neuron output. Moreover, our study suggests an intriguing link between basal process retention and the signaling triggered by basal lamina and related extracellular matrix proteins in that integrin function is shown here to be required for OSVZ-progenitor proliferation.

OSVZ-progenitors – a hallmark of a gyrencephalic cortex?

In a previous pioneering study[9] which provides the first description of the unique morphological features of the OSVZ, it was suggested that the OSVZ may be primate-specific. Our findings indicate that OSVZ-progenitors exist in a non-primate species, the ferret, which like primates develops a gyrencephalic cortex. Considering the previous[9] and present study together, the intriguing possibility arises that OSVZ-progenitors (delaminated RGCs retaining basal lamina contact, see below) as such may be characteristic of a developing gyrencephalic cortex, and that it is a quantitative rather than qualitative aspect, i.e. their relative abundance, which distinguishes the developing primate from the developing gyrencephalic non-primate cortex.

OSVZ-progenitors are delaminated epithelial-like RGCs

Like rodent BPs, human and ferret OSVZ-progenitors delaminate from the apical adherens junction belt, retract their apical process and down-regulate apical polarity markers. However, OSVZ-progenitors are strikingly different from the typical rodent BP in that they retain characteristic features of RGCs, that is, sustained expression of Pax6 and several cytoplasmic RGC markers[43] and, importantly, a basal process through M-phase. In line with previous considerations[9], OSVZ-progenitors can therefore be regarded as delaminated RGCs, a conclusion reported independently by Hansen et al.[44] while our manuscript was under review. Importantly, however, OSVZ-progenitors retain, via their basal process, cell polarity and a canonical epithelial feature – the contact with the basal lamina. The present findings therefore in principle support the epithelial progenitor hypothesis[4].

Basal polarity, asymmetric cell division and neuron output

However, given the down-regulation of apical polarity and loss of apical adherens junctions, OSVZ-progenitors apparently do not retain all possible epithelial features. It is interesting to note that concomitant with this loss, neural progenitors switch from a predominantly vertical (apical, VZ-progenitors) to a near-random, if not preferentially horizontal (basal, SVZ-progenitors), cleavage plane orientation. Symmetric proliferative divisions of polarized neural progenitors thus appear to be linked to the maintenance of bipolar (apical-basal) cell polarity (**Suppl. Fig. 4a** top), whereas the transition to monopolar (basal) cell polarity seems to confine neural progenitors to cell biologically asymmetric divisions (**Suppl. Fig. 4a** bottom right).

Rodent BPs in M-phase are unpolarized, and hence their divisions can only be symmetric (in cell biological terms) and do not require any particular control of cleavage plane orientation[8]. By contrast, APs show extreme apical-basal polarity, and hence for their

divisions to be symmetric (in cell biological terms), two requirements must be met; (i) the cleavage plane must be oriented perfectly parallel to the apical-basal cell axis, and (ii) the cleavage must divide apical and basal cell constituents[6]. Mechanisms to meet either requirement have been reported[4,21,45]. Our present findings that human OSVZ-progenitors, like mouse BPs, show a near-random cleavage plane orientation but, in contrast to the latter, retain basal polarity imply, when considered together, that OSVZ-progenitor divisions are cell biologically asymmetric. In other words, given that both rodent BPs and human/ferret OSVZ-progenitors show random cleavage plane orientation, the retention of the basal process in OSVZ-progenitors converts them from dividing symmetrically (as rodent BPs do (**Suppl. Fig. 4a** bottom left)) to dividing asymmetrically (**Suppl. Fig. 4a** bottom right).

Repeated asymmetric divisions not only of APs, but also of the OSVZ-progenitors generated therefrom, would considerably affect neuron output. The existence of BPs undergoing symmetric, neurogenic and self-consuming, divisions merely doubles neuron number (**Suppl. Fig. 4b** left). In contrast, repeated asymmetric, neurogenic and self-renewing, OSVZ-progenitor divisions would result in the progressive accumulation of neurons (**Suppl. Fig. 4b** right), outnumbering that in the AP-to-BP lineage (**Suppl. Fig. 4b** left).

Integrins on basal processes and OSVZ-progenitor expansion

Hence, the key question emerging is: why are OSVZ-progenitors, in contrast to most BPs in the rodent, capable of undergoing self-renewing divisions, as shown previously[23]. Our data suggest that the answer to this question lies in the cell biological difference between these two types of progenitors – the retention of the basal process. Stem cells in other epithelial systems, e.g. the skin, characteristically maintain basal lamina contact[46,47]. Moreover, the basal process has recently been implicated in the self-renewal of mouse APs[31]. Extrapolating from these studies, it is intriguing to hypothesize that OSVZ-progenitors

maintain stem cell-like properties via their basal process and the basal lamina contact it mediates.

One of the major signaling pathways via which basal lamina and related extracellular matrix proteins influence cell fate involves integrin receptors. Indeed, our data indicate that the function of integrins which are present in the basal process[39,40] is required for OSVZ-progenitor proliferation. Intriguingly, two independent forms of interference with integrin function selectively reduced the population size of ferret OSVZ-progenitors (Pax6-positive/Tbr2-negative), which were found to retain their basal process throughout the cell cycle, whereas no such effects were observed for the SVZ-progenitor subpopulation which lacked basal processes (Pax6-negative/Tbr2-positive). Given our observation that beta-3 integrins are concentrated at varicosities of the basal process of SVZ-progenitors, a plausible concept is that basal process retention serves to allow integrin-mediated self-renewal of SVZ-progenitors. This concept is not necessarily contradicted by the previous findings that perturbation of integrin function in mouse RGCs did not significantly impair their self-renewal[35], because the latter progenitors have access to potential proliferation signals from the ventricle, which OSVZ-progenitors do not. In conclusion, our study raises the possibility that basal process-based integrin function may play a key role in SVZ expansion during cortex evolution.

Acknowledgements

We thank Jussi Helppi and other members of the animal facility, and the light microscopy facility of MPI-CBG for excellent support, Drs. Anne-Marie Marzesco and Elena Taverna for experimental advice, Christiane Haffner for excellent technical assistance, Stephan Preibisch for developing the Fiji plug-in, and Dr. Jeremy Pulvers for his helpful comments on the manuscript. We are grateful to the Bundesinstitut für Risikobewertung, Berlin, and Biotie Therapies, Radebeul-Dresden, Germany, for ferret housing. S.A.F., I.K. and J.L.F. were members of the International Max Planck Research School for Molecular Cell Biology and Bioengineering. W.B.H. was supported by a grant from the DFG (SFB 655, A2), by the DFG-funded Center for Regenerative Therapies Dresden, and by the Fonds der Chemischen Industrie.

Author Contributions

S.A.F. performed the experiments on human tissue, contributed equally to the experiments on ferret tissue, and co-wrote the paper. I.K. contributed equally to the experiments on ferret tissue and co-wrote the paper. J.V. provided human tissue and gave advice on the experiments. M.W.-B. performed the EM analyses. D.S. proposed the use of echistatin and contributed to some experiments. D.C. provided reagents for prominin-1 analyses. J.L.F., A.R., W.D. and R.N. provided human tissue. W.B.H. supervised the project and wrote the paper.

Figure Legends

Fig. 1. Pax6 and Tbr2 expression in developing human and ferret neocortex.

(**a**–**c**) Quantification of Pax6-positive (Pax6+, grey) and Tbr2-positive (Tbr2+, black) mitoses, revealed by PH3 immunostaining, in the 10-16 w.p.c. VZ (**a**), SVZ (**b**), and the 16-w.p.c. ISVZ and OSVZ (**c**) of human fetal neocortex, expressed as percentage of total PH3-positive cells in the respective layer. See Supplementary Information (I) for cell numbers. Data for 10- and 12-w.p.c. are from one fetus, for 14- and 16-w.p.c. from two fetuses; bars indicate variation of individual values from the mean.

(**d**–**k**) Pax6 (red), Tbr2 (green) and DAPI (blue) staining on cryosections (**d**, **e**; PFA) and paraffin sections (**f**–**k**; formalin) of 10-16 w.p.c. human fetal neocortex. The basal boundary of the SVZ/OSVZ corresponds to the top margin of the images. Scale bars, 50 μm.

(**l**, **m**) Quantification of Pax6-positive (Pax6+, grey) and Tbr2-positive (Tbr2+, black) mitoses, revealed by PH3 immunostaining, in the VZ (**l**) and SVZ (**m**) of E32-P10 ferret neocortex, expressed as percentage of total PH3-positive cells in the respective layer. See Supplementary Information (I) for cell numbers. Data are from one developing ferret brain each.

(**n**–**s**) Pax6 (red), Tbr2 (green) and DAPI (blue) staining on cryosections of PFA-fixed E32-P10 ferret neocortex. Further specifications are as in (**d**–**k**).

Fig. 2. Human OSVZ-progenitors express markers of radial glia.

(**a**) Double immunofluorescence for nestin (red) and PH3 (green), combined with DAPI staining (blue), on a vibratome section of 11-w.p.c. human fetal neocortex (PFA); a portion of the SVZ is shown (stack of 8 optical sections). Arrowheads, mitotic SVZ-progenitor cell bodies showing nestin immunoreactivity. Scale bar, 10 μm.

(**b**, **c**) Immunofluorescence for BLBP (red), combined with DAPI staining (blue), on a vibratome section of 13-w.p.c. human fetal neocortex (PFA). Boxed areas in (**b**) are shown at higher magnification in (**c**); arrowheads, cell body-associated BLBP immunoreactivity in the SVZ and VZ. Scale bars, 50 μm (**b**), 10 μm (**c**).

(**d**–**g**) Immunofluorescence (red) for nestin combined with DAPI staining (blue) (**d**, **e**), for GLAST (**f**) and for GFAP (**g**) on paraffin sections of 16-w.p.c. human fetal neocortex (formalin). Boxed areas in (**d**) are shown at higher magnification in (**e**) and are representative of the areas shown in (**f**) and (**g**); arrowheads, cell body-associated immunoreactivity in the OSVZ and VZ. Scale bars, 50 μm (**d**), 10 μm (**e**–**g**).

Fig. 3. Human and ferret OSVZ-progenitors retain basal processes through M-phase.

(**a**–**g**) 13-w.p.c. human fetal neocortex (PFA); (**a**–**d**) vibratome sections, (**e**–**g**) cryosections; (**h**–**o**) E39 ferret neocortex (PFA, vibratome sections).

(**a**) DiI labeling (red) from the pial surface of the cortical wall, combined with DAPI staining (blue); stack of 28 optical sections. Solid arrowheads, DiI-labeled cell bodies; open arrowheads, DiI-labeled cellular processes; asterisks, autofluorescent blood vessels. The DAPI image corresponds to a segment of the DiI image. Scale bar, 50 μm.

(**h, i**) DiI labeling (red) from the pial surface of the cortical wall, combined with Ki67 immunofluorescence (**i**, green) and DAPI staining (**h**, blue); stack of 20 optical sections. The boxed area in (**h**) is shown at higher magnification (**i**); solid arrowhead, DiI-labeled Ki67-positive cell body; open arrowheads, DiI-labeled basal process. Scale bar, 50 μm (**h**), 20 μm (**i**).

(**b**, **c, j, k**) Immunofluorescence for phosphovimentin (pVim, red), combined with DAPI staining (blue); (**b**) human VZ, (**c**) human SVZ, (**j**) ferret VZ, (**k**) ferret SVZ (stacks of 6-12 optical sections). Arrowheads, phosphovimentin-positive basal processes. Scale bars, 5 μm.

(**d, l**) Quantification of the percentage of mitotic progenitors, identified by phosphovimentin immunostaining, in the human (**d**) and ferret (**l**) VZ (grey columns) and SVZ (black columns) that show phosphovimentin-positive basal processes. See Supplementary Information (I) for cell numbers. Data are from one human fetus and one ferret embryo.

(**e**, **f, m, n**) Double immunofluorescence for phosphovimentin (pVim, red) and either Pax6 (**e**, **m**, green) or Tbr2 (**f**, **n**, green) of SVZ-progenitors (stacks of 5-8 optical sections). Solid arrowheads in (**e, m**), Pax6-positive mitotic human (**e**) and ferret (**m**) SVZ-progenitor extending a basal process; open arrowheads in (**f, n**), Tbr2-negative mitotic human (**f**) and ferret (**n**) SVZ-progenitor extending a basal process. Scale bars, 5 μm.

(**g, o**) Quantification of the percentage of mitotic, basal process-bearing human (**g**) and ferret (**o**) SVZ-progenitors, identified by phosphovimentin immunostaining, that show either Pax6 (Pax6+) or Tbr2 (Tbr2+) expression. See Supplementary Information (I) for cell numbers. Data are from one human fetus and one ferret embryo.

Fig. 4. Human OSVZ-progenitors show perinuclear centrosomes.

(**a**–**c**) Immunofluorescence for γ-tubulin (red), combined with DAPI staining (blue), on a cryosection of formalin-fixed 17-w.p.c. human fetal neocortex; (**a, b, c** OSVZ and ISVZ) stack of 10 optical sections, (**c** VZ) stack of two optical sections. The DAPI image (**a**) corresponds to a segment of the immunofluorescence image (**b**). Boxed areas in (**b**) are shown at higher magnification in (**c** OSVZ) and (**c** ISVZ), along with a higher magnification of the VZ (**c** VZ). Asterisks, autofluorescent blood vessels. Scale bars, 50 μm (**a**, **b**), 5 μm (**c**).

(**d**–**g**) EM of 17-w.p.c. human fetal neocortex. (**d**) Nucleus and perinuclear area of an OSVZ-progenitor with a perinuclear centrosome. The boxed area containing the centrosome is shown at higher magnification in (**e**, arrowhead). (**f**) Ventricular surface showing the apical region of several VZ-progenitors. Arrows indicate adherens junctions, the distance between which was

measured to determine the average apical width (**Table 1**); arrowheads, centrosomes. The boxed area containing a centrosome between adherens junctions is shown at higher magnification in (**g**). The ventricular surface is down in (**f**, **g**). Scale bars, 1 μm (**d**, **f**) and 200 nm (**e**, **g**).

Fig. 5. Human and ferret SVZ-progenitors show near-random cleavage plane orientation resulting in asymmetric inheritance of the basal process.

(**a**) DAPI staining of paraffin sections of 14-w.p.c. (OSVZ, VZ) and 16-w.p.c. (ISVZ) human fetal neocortex (formalin), showing sister chromatids of progenitors in anaphase/early telophase (arrowheads) in the OSVZ, ISVZ and VZ (stacks of 4-8 optical sections). Scale bars, 20 μm.

(**b, c, h, i**) Quantification of cleavage plane orientation of progenitors in anaphase/early telophase. Cleavage plane orientations were grouped into three categories, 0-30° (white), 30-60° (grey) and 60-90° (black), with 0° corresponding to an orientation parallel to the ventricular surface. (**b**) Total progenitors in OSVZ, ISVZ and VZ, and (**c**) Pax6-positive (Pax6+) and Tbr2-positive (Tbr2+) SVZ-progenitors, in 14-16–w.p.c. human neocortex (paraffin sections); (**h**) total progenitors in SVZ and VZ, and (**i**) Pax6+ and Tbr2+ SVZ-progenitors, in E39 ferret neocortex (PFA). See Supplementary Information (I) for cell numbers.

(**d**–**g**, **j**, **k**) Immunofluorescence for phosphovimentin (pVim, red) combined with DAPI staining (blue) on a vibratome section (**d**), and double immunofluorescence for phosphovimentin (pVim, red) and Aurora B (green) on cryosections (**e**–**g**, **j**, **k**), of 13-w.p.c. fetal human (**d**–**g**) and E39 ferret (**j**, **k**) neocortex (PFA, stacks of 4-12 optical sections). Dashed circle in (**d**), DAPI-stained sister chromatids in anaphase; solid arrowheads,

phosphovimentin-positive basal processes; arrows, midbodies; open arrowheads, a phosphovimentin-positive apical process. Scale bars, 5 μm.

Fig. 6. Inhibition of integrin function decreases the population of cycling Pax6-positive/Tbr2-negative SVZ-progenitors, but not of cycling Pax6-negative or Tbr2-positive SVZ-progenitors, in the E40 ferret neocortex.

(**a**–**n**) Slice cultures of E40 ferret telencephalon were incubated for up to 96 hours in the absence (Control: **a**, **c**; **e**–**n** light-grey columns) or presence of 4 μM echistatin (Echistatin: **b**, **d**; **f**–**n** black columns) or 25 μg/ml αvβ3 integrin blocking antibody (αvβ3 Ab: **e**, dark-grey columns), followed by double immunofluorescence and quantification of progenitor populations at the indicated time points (**e**, 96 hours).

(**a**–**d**) Double immunofluorescence after 96 hours of culture for Ki67 (green) and either Tbr2 (**a**, **b**; red) or Pax6 (**c**, **d**; red), each combined with DAPI staining (blue). The top margin of the images corresponds to the transition zone subplate/cortical plate. Scale bars, 50 μm.

(**e**–**n**) Quantification of Ki67-positive (Ki67+) progenitor populations, each expressed for a unit area of 1 mm^2 of cortical wall either from the ventricular surface (**f**–**j,** VZ + SVZ) or from from the VZ/SVZ boundary (**e**, **k**–**n,** SVZ) to the beginning of the cortical plate; total Ki67+ progenitors (**e**, **f**, **l**), Ki67+ progenitors showing Pax6 immunoreactivity (Pax6+/Ki67+, **e**, **i**, **k**), Ki67+ progenitors lacking Pax6 immunoreactivity (Pax6–/Ki67+, **e**, **j**), Ki67+ progenitors showing Tbr2 immunoreactivity (Tbr2+/Ki67+, **g**, **m**), Ki67+ progenitors lacking Tbr2 immunoreactivity (Tbr2–/Ki67+, **e**, **h**, **n**); (**f**) are data from double immunofluorescence for Tbr2, (**l**) are data from double immunofluorescence for Pax6. See Supplementary Information (I) for image numbers. Bars indicate SEM; single asterisk, $p < 0.05$; double asterisk, $p < 0.01$; triple asterisk, $p < 0.001$).

Fig. 7. Localization of beta-3-integrin on basal processes of ferret SVZ- and VZ-progenitors

(**a**–**d**) Double immunofluorescence for phosphovimentin (pVim, red) and beta-3-integrin (b3-int, green) on cryosections of E39 ferret neocortex, showing mitotic, basal process-bearing SVZ-progenitors (**a**, **b**) and VZ-progenitors (**c**, **d**). Note the integrin immunoreactivity at varicosities of the basal process (arrowheads). Scale bar, 5 μm.

Materials and Methods

Tissue

HUMAN FETAL BRAIN. Human fetal brain tissue was obtained from the Institut für Zell- und Neurobiologie, Centrum für Anatomie, Charité, Berlin, and the Klinik und Poliklinik für Frauenheilkunde und Geburtshilfe, Universitätsklinikum Carl Gustav Carus of the Technische Universität Dresden, Germany. The age of the human fetuses ranged from 10 to 17 weeks post-conception (p.c.) (10 weeks p.c., n=1; 11 weeks p.c., n=1; 12 weeks p.c., n=1; 13 weeks p.c., n=1; 14 weeks p.c., n=2; 16 weeks p.c., n=2; 17 weeks p.c., n=1), as assessed by ultrasound measurements of crown-rump length and other standard criteria of developmental stage determination. Pregnancies were terminated on the basis of social or medical indications. In the case of the latter, only medical indications not known to affect brain development (e.g., amnion infection) were included in the present study. Human fetal brain tissue was obtained with informed written maternal consent, with approval of the local University Hospital Ethical Review Committees. Human fetuses were placed at 4°C immediately after abortion, and brains were dissected in ice-cold PBS and fixed for at least 24 h at 4°C in either 4% paraformaldehyde (PFA) in 120 mM phosphate buffer pH 7.4 (for

cryosections and vibratome sections) or 4% formalin in 100 mM phosphate buffer pH 7.4 (for paraffin sections, cryosections and vibratome sections), as indicated in the figures legends.

FERRET EMBRYONIC AND POSTNATAL BRAIN. Timed-pregnant ferrets were obtained from Marshall BioResources (North Rose, NY, USA) and housed at the Bundesinstitut für Risikobewertung, Berlin, or at Biotie Therapies, Radebeul-Dresden, Germany. At embryonic day (E) 32, 39 or 40, pregnant ferrets were anesthetized by intramuscular injection of ketamine (20 mg/kg, Bela-Pharm) plus xylazine (1 mg/kg, Pharma-Partner) and sacrificed by intracardiac injection of T-61 (0.3 ml/kg, Intervet) followed by the immediate removal of embryos and dissection of the brains in ice-cold PBS. Postnatal day (P) 10 ferrets were anesthetized by intraperitoneal injection of ketamine plus xylazine as above and sacrificed by decapitation, followed by dissection of the brains. Embryonic and postnatal ferret brains were fixed in 4% PFA as above (E32, E39, P10) or used for the preparation of slice cultures (E40) as described below. All animal experiments were performed in accordance with German animal welfare legislation and were approved by the Landesamt für Gesundheit und Soziales Berlin and the Landesdirektion Dresden.

Organotypic ferret cortical slice culture

E40 ferrets were dissected in Tyrode's solution at 4°C. Brains were embedded in 3% low-melting agarose (Invitrogen, UltraPure™) in PBS and again cooled to 4°C for vibratome sectioning. Sections (500 μm) of telencephalon were immersed at 4°C in 1 ml each of 1.5 mg/ml type Ia collagen (Cellmatrix, Nitta Gelatin) in DMEM in a 35-mm glass-bottom microwell dish (MatTek Corporation). Dishes were incubated for 5-10 min at 37°C to allow the collagen to solidify, transferred to a humidified POC-Chamber-System gassed with 40% O_2, 5% CO_2, 55% N_2 at 37°C, and incubated for further 30 min followed by addition of 2 ml of Neurobasal medium (Invitrogen) supplemented with 10% heat-inactivated horse serum

(Sigma), 1x N2 supplement (Invitrogen), 1x B27 supplement (Invitrogen), 2 mM L-glutamine, and 100 U/ml penicillin/streptomycin, which defined the start of culture. In the case of perturbation of integrin signaling, 4 μM echistatin[42] (Sigma) or 25 μg/ml αvβ3 integrin blocking antibody (Millipore, MAB1976Z) was added to both, the collagen/DMEM and the culture medium. Medium was changed after 48 hours. The collagen-embedded sections were fixed by addition of 4% PFA in PBS for 24 h at 4°C, followed by removal of the sections from the collagen, infiltration with 30% sucrose for 48 h at room temperature, and processing for cryosectioning and immunocytochemistry as described below.

Immunocytochemistry

Human and ferret telencephalon was sectioned. For cryosectioning, fixed brain tissue was infiltrated with 30% sucrose in PBS overnight at 4°C (except for E40 ferret slices) and then embedded in Tissue-Tek (Sakura Finetek) and stored at -20°C. Cryostat sections were cut at 12-14 μm, except for E40 ferret slice cultures which were cut at 16 μm. For vibratome sectioning, fixed brain tissue was embedded in 3% low-melting agarose in PBS, cut at 50 μm and stored in PBS at 4°C until further processing. For microtome sectioning, formalin-fixed brain tissue was dehydrated in graded ethanol solutions followed by xylene or chloroform, and then embedded in paraffin. Paraffin sections were cut at 12 μm, dewaxed in xylene and rehydrated in graded ethanol solutions. All sections were subjected to an antigen retrieval protocol. Cryosections and paraffin sections on glass slides were boiled for 1 min in a microwave oven at 800 W in citrate buffer pH 6 (Target Retrieval Solution, DakoCytomation) followed by 10 min at 80 W, floating vibratome sections were heated in the same buffer for 30 min at 85°C. Sections were then permeabilized with 0.3% Triton X-100, quenched with 0.1 M glycine and then subjected to immunocytochemistry according to standard procedures[27]. Primary antibodies were incubated overnight (cryosections, vibratome sections)

or for 1.5 days (paraffin sections) at 4°C, secondary antibodies for 1 hour at room temperature. The following primary antibodies were used: rabbit antibodies against Pax6 (Covance, PRB-278P, 1:200 for cryosections, 1:50 for paraffin sections), Tbr2 (Abcam, ab23345, 1:200 for cryosections, 1:50 for paraffin sections), phosphohistone H3 (Millipore, 06-570, 1:200) conjugated to DyLight 633 (Thermo Scientific), nestin (Abcam, ab5968, 1:200), BLBP (Santa Cruz, sc-30088, 1:200), Par3 (Millipore, 07-330, 1:50), GLAST (Invitrogen, 428100, 1:200), Aurora B (Abcam, ab2254, 1:200), integrin beta 3 (Abcam, ab75872, 1:200); mouse mAbs against human prominin-1 (80B258[48], 8.7 ng/µl), aPKC (BD Transduction Laboratories, 610207, 1:100), ZO-1 (Invitrogen, 33-9100, 1:200), Ki67 antigen (DakoCytomation, M 7240, 1:200), GFAP (Sigma, G3893, 1:200), GLAST (Abcam, ab49643, 1:200), phosphovimentin (Abcam, ab22651, 1:50; MBL, D076-3, 1:50). Goat Cy2-, Cy3-, Cy5-labeled secondary antibodies (Jackson Laboratories) were used (1:500). All sections were counterstained with DAPI (Sigma, 1:500) and mounted in Mowiol (Merck Biosciences).

DiI labeling

Human and ferret vibratome sections of PFA-fixed telencephalon were kept in 35-mm plastic microwell dishes (Nunc) in PBS and immobilised using a metal grid (diameter 1 cm) with nylon wires (Warner Instruments). DiI suspension (1,1'-dioctadecyl—3, 3, 3', 3'-tetramethylindocarbocyanine perchlorate, 10 µg/µl in ethanol, Molecular Probes) was applied to the section locally at the apical or basal side of the cortical wall using a glass capillary (0.5-1 µm opening) and an Eppendorf Transjector (model 5246) attached to an InjectMan NI2 micromanipulator under microscopic control (Axiovert 200, Zeiss). Sections were incubated for 5 d at 37°C. Sections were then heated in citrate buffer pH 6 (Target Retrieval Solution,

DakoCytomation) for 30 min at 85°C, quenched with 0.1 M glycine and then subjected to immunocytochemistry as described above except that Triton X-100 was omitted throughout.

In situ hybridization

In-situ-hybridization for human prominin-1 was performed according to standard methods, using cryosections and digoxigenin-labeled (DIG-RNA labeling kit, Roche) cRNA antisense and sense probes corresponding to the first 275 nucleotides of the open reading frame[49] at 100 ng/ml.

Image acquisition

Fluorescence and in-situ hybridization images were acquired using a Zeiss 510 confocal laser-scanning microscope or an Olympus IX-71 wide-field microscope, using 20× or 40× objectives with either microscope. Images were acquired as 1-µm single optical sections, and unless indicated otherwise in the figure legends, all panels shown are single 1-µm optical sections. Single images were stitched together using Fiji software and a plug-in[50]. All images were processed using Photoshop software (Adobe). All images are oriented with the ventricular surface down or with the bottom margin towards the ventricular surface.

Electron Microscopy

For electron microscopical analysis, a vibratome section of formalin-fixed 17-weeks p.c. human telencephalon was postfixed in 2.5% glutaraldehyde in 0.1 M sodium phosphate buffer (pH 7.4) and subsequently in 1% osmium tetroxide prior to embedding in EmBed-812 (Science Services) according to standard procedures. Ultrathin 200-nm sections were cut on a Leica UCT ultramicrotome (Leica Microsystems), poststained with uranyl acetate and lead

citrate and viewed in a Tecnai 12 electron microscope (FEI company). Images were taken with a Tietz F214 camera (TVIPS).

Quantification of centrosomes

For quantification of the occurrence of centrosomes in VZ and OSVZ cells in interphase, EM images were analyzed as follows. The average width of the apical process of a cell contacting the ventricle (VZ single-cell apical region) was defined as the distance between the apical-most features of cross-sectioned adherens junctions. The average width of the perinuclear region of an OSVZ cell (OSVZ perinuclear region) was defined as the diameter of their elongated, radially aligned nucleus perpendicular to the radial axis, assuming a negligible contribution of cytoplasm to the cell width. These distance measurements were performed using iTEM software (Olympus). The resulting values were used to calculate the average number of 200-nm sections that would be required to cover a VZ single-cell apical region and an OSVZ perinuclear region. We assumed a centrosome size of ≥400 nm, which implies that a centrosome appears in three 200-nm sections (as a 400-nm centrosome will only rarely be contained in just two 200-nm sections).

Determination of cleavage plane orientation

Cleavage plane orientation of progenitors in the VZ, ISVZ and OSVZ was deduced from the position of the DAPI-stained sister chromatids in anaphase or early telophase[27] and was expressed relative to the ventricular surface, with a cleavage plane parallel to the ventricular surface being defined as 0°.

Quantifications and statistical analysis

In the case of 16- and 17-week p.c. human neocortex, the basal-most region of the VZ and the apical-most region of the OSVZ were distinguished from the interjacent ISVZ by the shape of DAPI-stained nuclei (radially elongated shape and radial orientation in the VZ and OSVZ, spherical shape in the ISVZ[9]). The same criteria were applied to determine the boundary between the 10-14-week p.c. human and E32-P10 ferret VZ (elongated nuclei) and SVZ (spherical nuclei). Quantification of cells for the parameters indicated was performed using Photoshop and ImageJ or Fiji software. The length of ventricular surface was determined by tracing it using ImageJ or Fiji software. For the determination of cortical wall area (excluding the cortical plate), a polygon was constructed using Image J and its area was calculated; the bottom and top side of the polygon corresponded to the traced ventricular surface and a straight line at the transition of the subplate to cortical plate, respectively, with the left and right side being two parallel straight lines in the radial axis of the cortical wall.

Statistical significance was calculated using Student's t-test.

References

1. Kriegstein, A., Noctor, S. & Martínez-Cerdeño, V. Patterns of neural stem and progenitor cell division may underlie evolutionary cortical expansion. *Nat Rev Neurosci* **7**, 883-890 (2006).
2. Molnár, Z.*, et al.* Comparative aspects of cerebral cortical development. *Eur J Neurosci* **23**, 921-934 (2006).
3. Abdel-Mannan, O., Cheung, A.F. & Molnár, Z. Evolution of cortical neurogenesis. *Brain Res Bull* **75**, 398-404 (2008).
4. Fish, J.L., Kennedy, H., Dehay, C. & Huttner, W.B. Making bigger brains - the evolution of neural-progenitor-cell division. *J. Cell Sci.* **121**, 2783-2793 (2008).
5. Rakic, P. Evolution of the neocortex: a perspective from developmental biology. *Nat Rev Neurosci* **10**, 724-735 (2009).
6. Götz, M. & Huttner, W.B. The cell biology of neurogenesis. *Nat Rev Mol Cell Biol* **6**, 777-788 (2005).
7. Kriegstein, A. & Alvarez-Buylla, A. The glial nature of embryonic and adult neural stem cells. *Annu Rev Neurosci* **32**, 149-184 (2009).
8. Attardo, A., Calegari, F., Haubensak, W., Wilsch-Bräuninger, M. & Huttner, W.B. Live imaging at the onset of cortical neurogenesis reveals differential appearance of the neuronal phenotype in apical versus basal progenitor progeny. *PLoS ONE* **3**, e2388 (2008).
9. Smart, I.H., Dehay, C., Giroud, P., Berland, M. & Kennedy, H. Unique morphological features of the proliferative zones and postmitotic compartments of the neural epithelium giving rise to striate and extrastriate cortex in the monkey. *Cereb Cortex* **12**, 37-53. (2002).
10. Murphy, W.J., Pringle, T.H., Crider, T.A., Springer, M.S. & Miller, W. Using genomic data to unravel the root of the placental mammal phylogeny. *Genome Res* **17**, 413-421 (2007).
11. Englund, C.*, et al.* Pax6, Tbr2, and Tbr1 are expressed sequentially by radial glia, intermediate progenitor cells, and postmitotic neurons in developing neocortex. *J Neurosci* **25**, 247-251 (2005).
12. Kowalczyk, T.*, et al.* Intermediate Neuronal Progenitors (Basal Progenitors) Produce Pyramidal-Projection Neurons for All Layers of Cerebral Cortex. *Cereb Cortex* **19**, 2439-2450 (2009).
13. Bayatti, N.*, et al.* A Molecular Neuroanatomical Study of the Developing Human Neocortex from 8 to 17 Postconceptional Weeks Revealing the Early Differentiation of the Subplate and Subventricular Zone. *Cereb Cortex* **18**, 1536-1548 (2007).
14. Götz, M., Stoykova, A. & Gruss, P. Pax6 controls radial glia differentiation in the cerebral cortex. *Neuron* **21**, 1031-1044. (1998).
15. Mo, Z. & Zecevic, N. Is Pax6 Critical for Neurogenesis in the Human Fetal Brain? *Cereb Cortex* **18**, 1455-1465 (2007).
16. Carney, R.S., Bystron, I., Lopez-Bendito, G. & Molnár, Z. Comparative analysis of extra-ventricular mitoses at early stages of cortical development in rat and human. *Brain Struct Funct* **212**, 37-54 (2007).
17. Kriegstein, A.R. & Götz, M. Radial glia diversity: a matter of cell fate. *Glia* **43**, 37-43 (2003).

18. Levitt, P. & Rakic, P. Immunoperoxidase localization of glial fibrillary acidic protein in radial glial cells and astrocytes of the developing rhesus monkey brain. *Journal Of Comparative Neurology* **193**, 815-840 (1980).
19. Woodhams, P.L., Bascó, E., Hajós, F., Csillág, A. & Balázs, R. Radial glia in the developing mouse cerebral cortex and hippocampus. *Anat Embryol (Berl)* **163**, 331-343 (1981).
20. Miyata, T., Kawaguchi, A., Okano, H. & Ogawa, M. Asymmetric inheritance of radial glial fibers by cortical neurons. *Neuron* **31**, 727-741 (2001).
21. Kosodo, Y.*, et al.* Cytokinesis of neuroepithelial cells can divide their basal process before anaphase. *EMBO J* **27**, 3151-3163 (2008).
22. Noctor, S.C., Martínez-Cerdeño, V. & Kriegstein, A.R. Distinct behaviors of neural stem and progenitor cells underlie cortical neurogenesis. *J Comp Neurol* **508**, 28-44 (2008).
23. Lukaszewicz, A.*, et al.* G1 phase regulation, area-specific cell cycle control, and cytoarchitectonics in the primate cortex. *Neuron* **47**, 353-364 (2005).
24. Kamei, Y.*, et al.* Visualization of mitotic radial glial lineage cells in the developing rat brain by Cdc2 kinase-phosphorylated vimentin. *Glia* **23**, 191-199 (1998).
25. Weigmann, A., Corbeil, D., Hellwig, A. & Huttner, W.B. Prominin, a novel microvilli-specific polytopic membrane protein of the apical surface of epithelial cells, is targeted to plasmalemmal protrusions of non-epithelial cells. *Proc. Natl. Acad. Sci. USA* **94**, 12425-12430 (1997).
26. Manabe, N.*, et al.* Association of ASIP/mPAR-3 with adherens junctions of mouse neuroepithelial cells. *Dev Dyn* **225**, 61-69. (2002).
27. Kosodo, Y.*, et al.* Asymmetric distribution of the apical plasma membrane during neurogenic divisions of mammalian neuroepithelial cells. *EMBO J.* **23**, 2314-2324 (2004).
28. Costa, M.R., Wen, G., Lepier, A., Schroeder, T. & Götz, M. Par-complex proteins promote proliferative progenitor divisions in the developing mouse cerebral cortex. *Development* **135**, 11-22 (2008).
29. Aaku-Saraste, E., Hellwig, A. & Huttner, W.B. Loss of occludin and functional tight junctions, but not ZO-1, during neural tube closure - remodeling of the neuroepithelium prior to neurogenesis. *Dev. Biol.* **180**, 664-679 (1996).
30. Chenn, A., Zhang, Y.A., Chang, B.T. & McConnell, S.K. Intrinsic polarity of mammalian neuroepithelial cells. *Mol Cell Neurosci* **11**, 183-193. (1998).
31. Konno, D.*, et al.* Neuroepithelial progenitors undergo LGN-dependent planar divisions to maintain self-renewability during mammalian neurogenesis. *Nat Cell Biol* **10**, 93-101 (2008).
32. Smart, I.H. & McSherry, G.M. Gyrus formation in the cerebral cortex in the ferret. I. Description of the external changes. *J Anat* **146**, 141-152. (1986).
33. Neal, J.*, et al.* Insights into the gyrification of developing ferret brain by magnetic resonance imaging. *J Anat* **210**, 66-77 (2007).
34. Schmid, R.S. & Anton, E.S. Role of integrins in the development of the cerebral cortex. *Cereb Cortex* **13**, 219-224 (2003).
35. Haubst, N., Georges-Labouesse, E., De Arcangelis, A., Mayer, U. & Gotz, M. Basement membrane attachment is dispensable for radial glial cell fate and for proliferation, but affects positioning of neuronal subtypes. *Development* **133**, 3245-3254 (2006).
36. Lathia, J.D., Rao, M.S., Mattson, M.P. & Ffrench-Constant, C. The microenvironment of the embryonic neural stem cell: lessons from adult niches? *Dev Dyn* **236**, 3267-3282 (2007).
37. Radakovits, R., Barros, C.S., Belvindrah, R., Patton, B. & Müller, U. Regulation of radial glial survival by signals from the meninges. *J Neurosci* **29**, 7694-7705 (2009).

38. Calvete, J.J., *et al.* Snake venom disintegrins: evolution of structure and function. *Toxicon* **45**, 1063-1074 (2005).
39. Hirsch, E., *et al.* Alpha v integrin subunit is predominantly located in nervous tissue and skeletal muscle during mouse development. *Dev Dyn* **201**, 108-120 (1994).
40. Yoshida, N., *et al.* Decrease in expression of alpha 5 beta 1 integrin during neuronal differentiation of cortical progenitor cells. *Exp Cell Res* **287**, 262-271 (2003).
41. Wierzbicka-Patynowski, I., *et al.* Structural requirements of echistatin for the recognition of alpha(v)beta(3) and alpha(5)beta(1) integrins. *J Biol Chem* **274**, 37809-37814 (1999).
42. Flanagan, L.A., Rebaza, L.M., Derzic, S., Schwartz, P.H. & Monuki, E.S. Regulation of human neural precursor cells by laminin and integrins. *J Neurosci Res* **83**, 845-856 (2006).
43. Middeldorp, J., *et al.* GFAPdelta in radial glia and subventricular zone progenitors in the developing human cortex. *Development* **137**, 313-321 (2010).
44. Hansen, D.V., Lui, J.H., Parker, P.R. & Kriegstein, A.R. Neurogenic radial glia in the outer subventricular zone of human neocortex. *Nature* **464**, 554-561 (2010).
45. Fish, J.L., Kosodo, Y., Enard, W., Pääbo, S. & Huttner, W.B. Aspm specifically maintains symmetric proliferative divisions of neuroepithelial cells. *Proc Natl Acad Sci U S A* **103**, 10438-10443 (2006).
46. Lechler, T. & Fuchs, E. Asymmetric cell divisions promote stratification and differentiation of mammalian skin. *Nature* **437**, 275-280 (2005).
47. Fuchs, E. Finding one's niche in the skin. *Cell Stem Cell* **4**, 499-502 (2009).
48. Karbanova, J., *et al.* The stem cell marker CD133 (Prominin-1) is expressed in various human glandular epithelia. *J Histochem Cytochem* **56**, 977-993 (2008).
49. Giebel, B., *et al.* Segregation of lipid raft markers including CD133 in polarized human hematopoietic stem and progenitor cells. *Blood* **104**, 2332-2338 (2004).
50. Preibisch, S., Saalfeld, S. & Tomancak, P. Globally optimal stitching of tiled 3D microscopic image acquisitions. *Bioinformatics* **25**, 1463-1465 (2009).

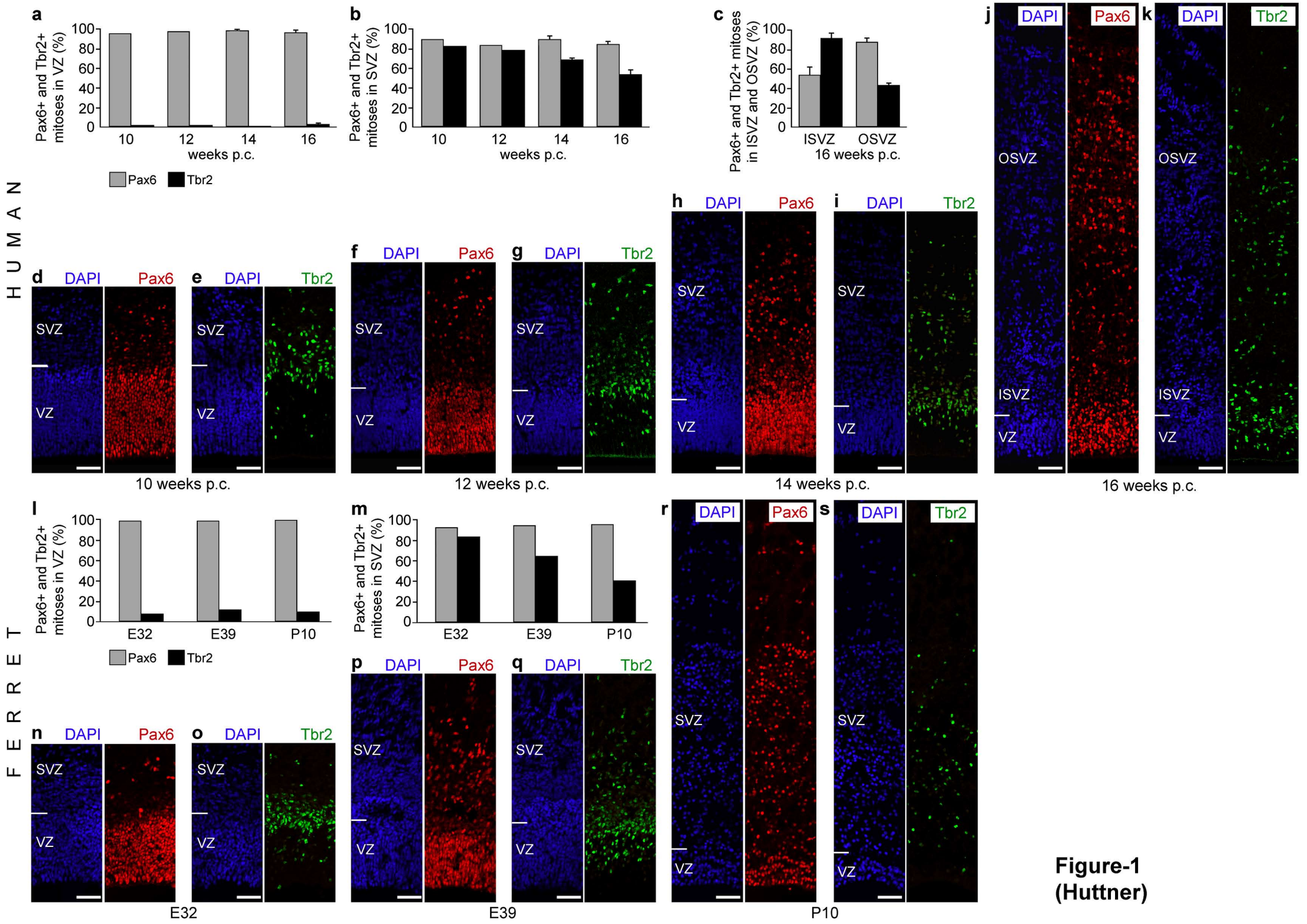

Figure-1 (Huttner)

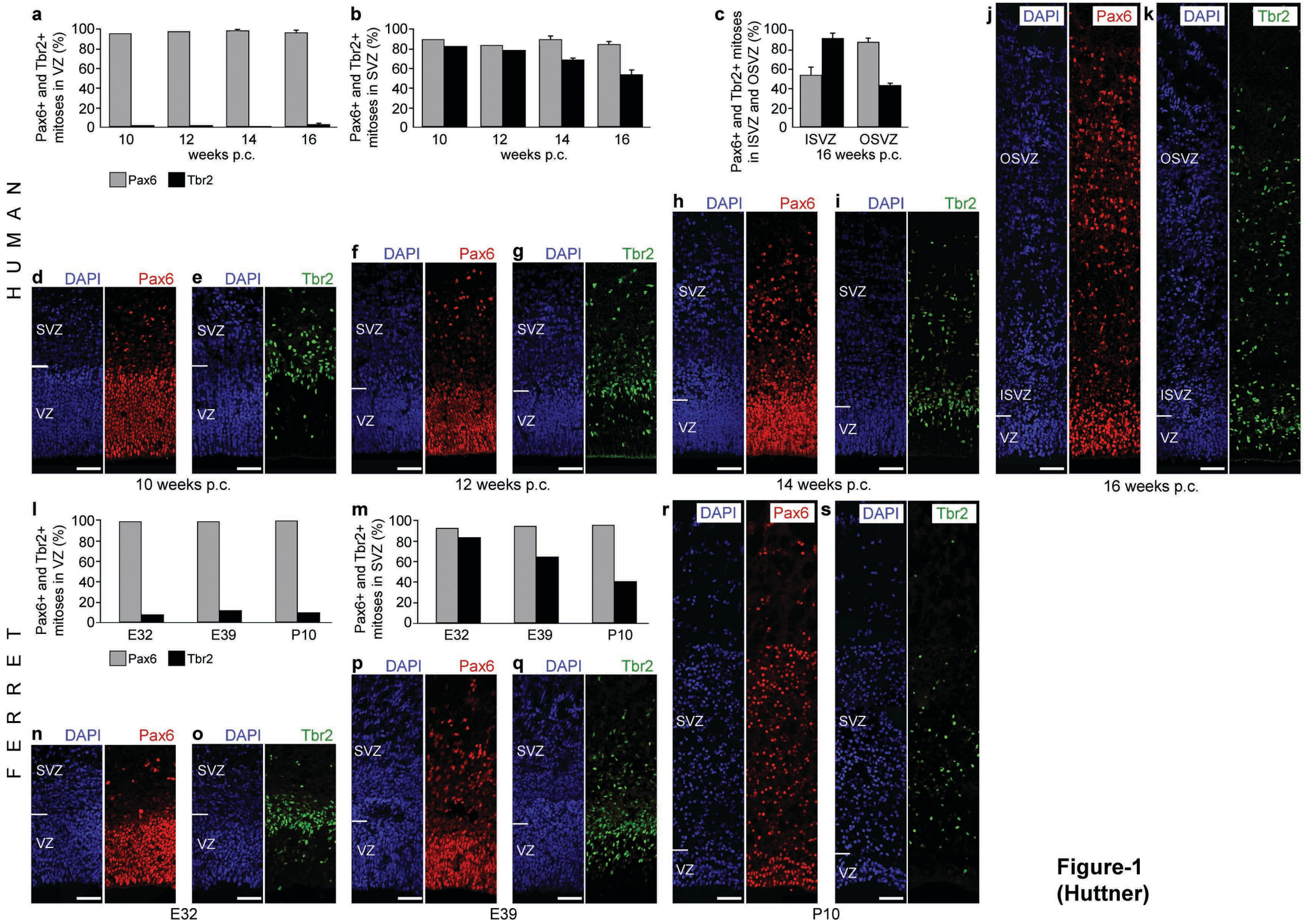

Figure-1 (Huttner)

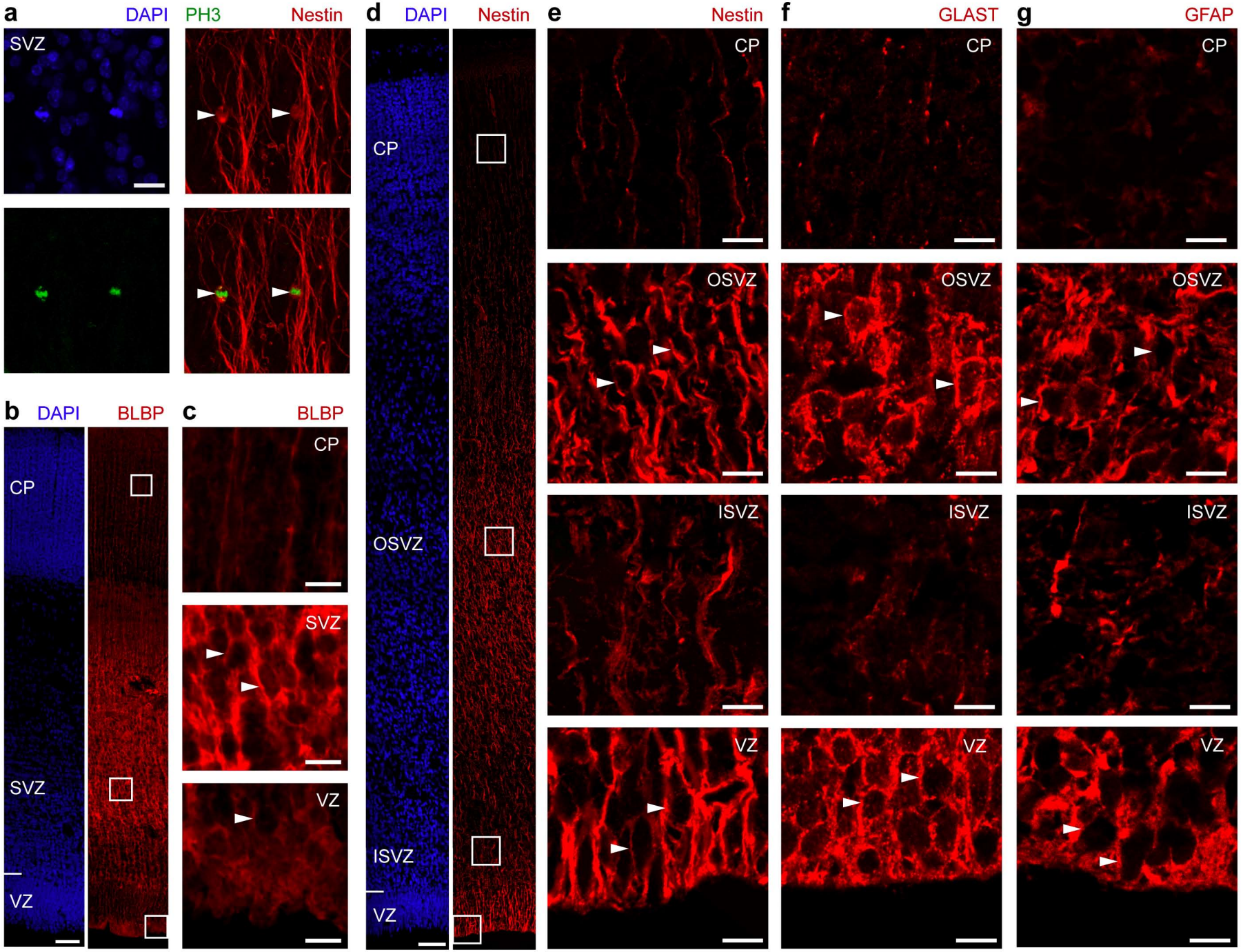

Figure-2 (Huttner)

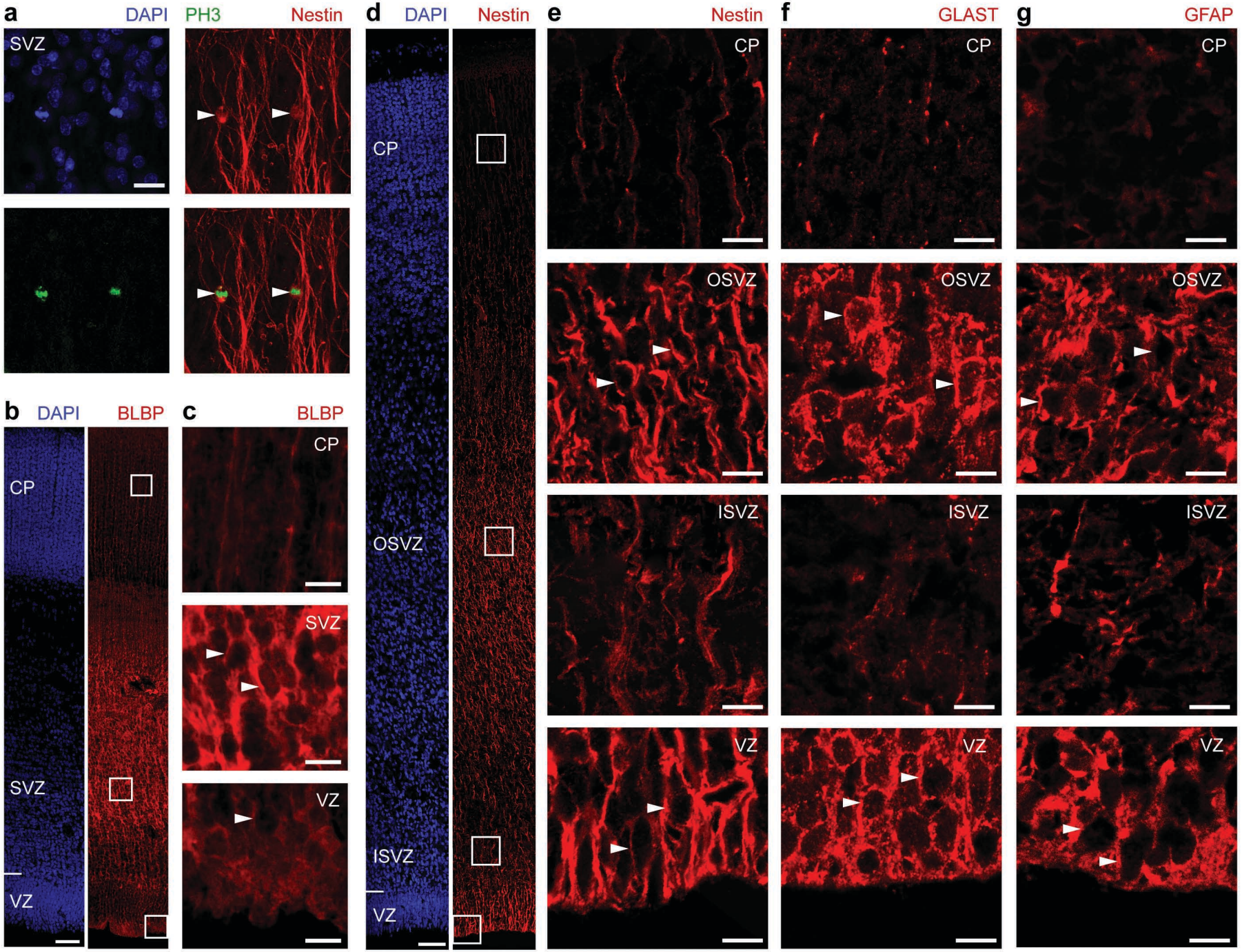

Figure-2 (Huttner)

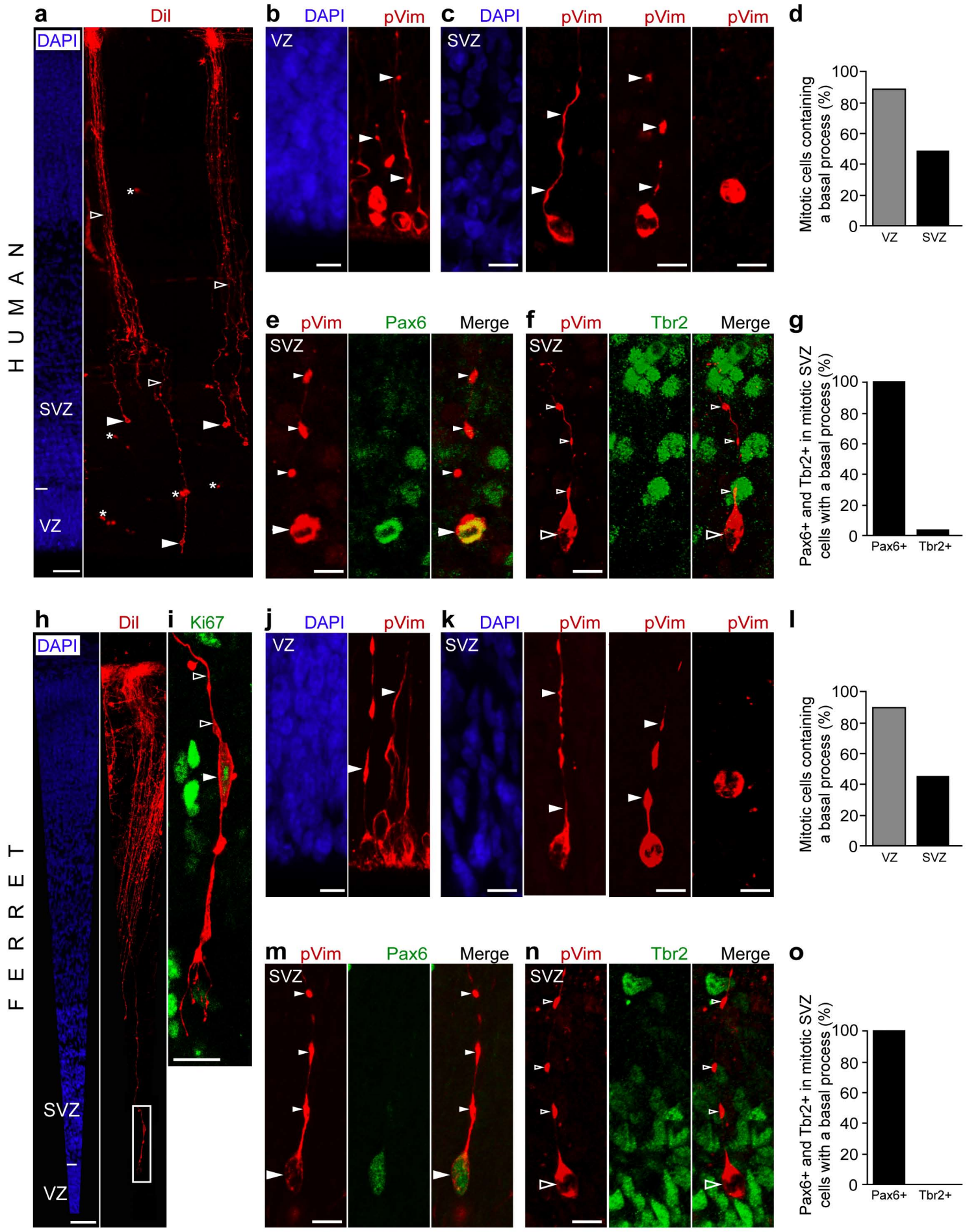

Figure-3 (Huttner)

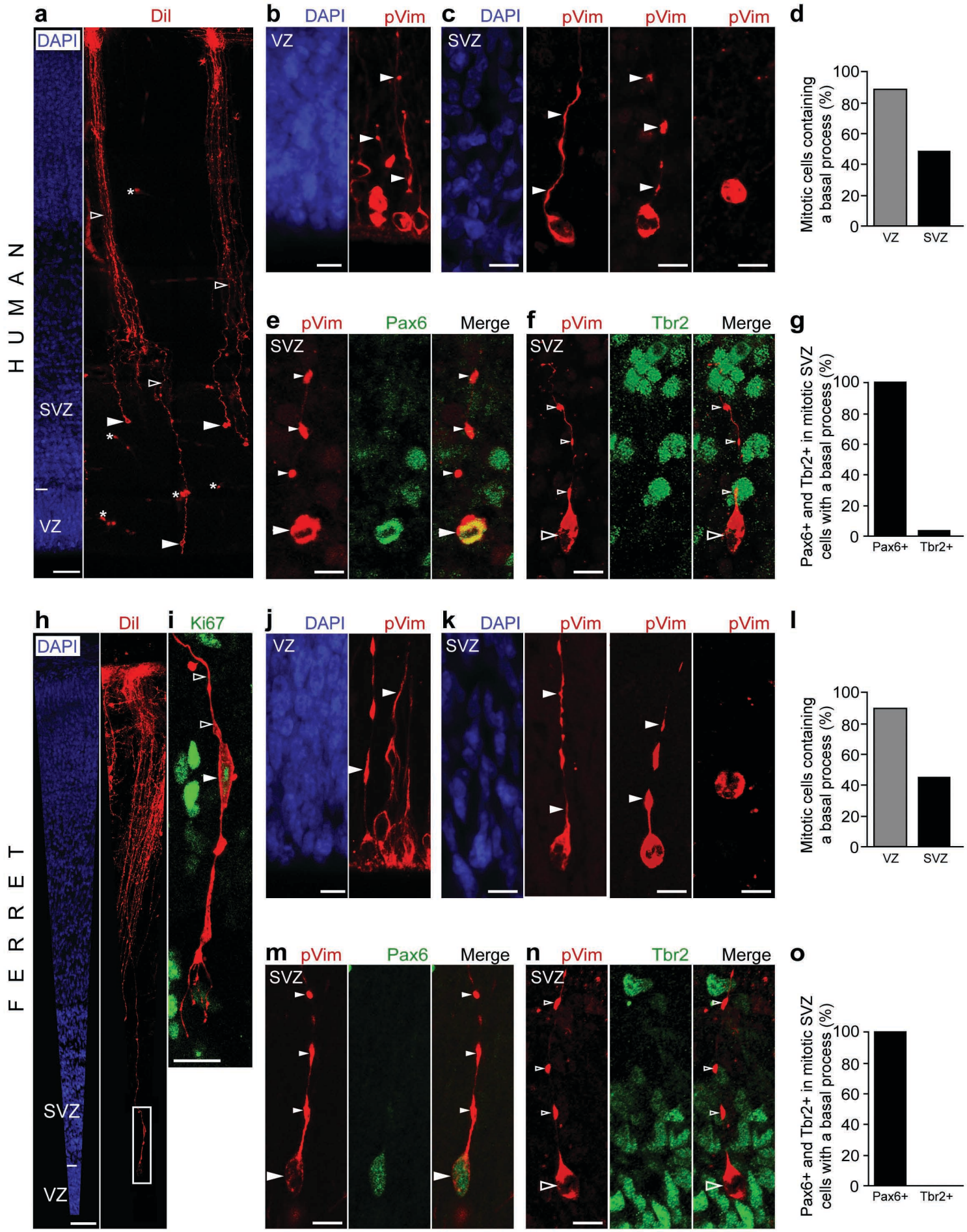

Figure-3 (Huttner)

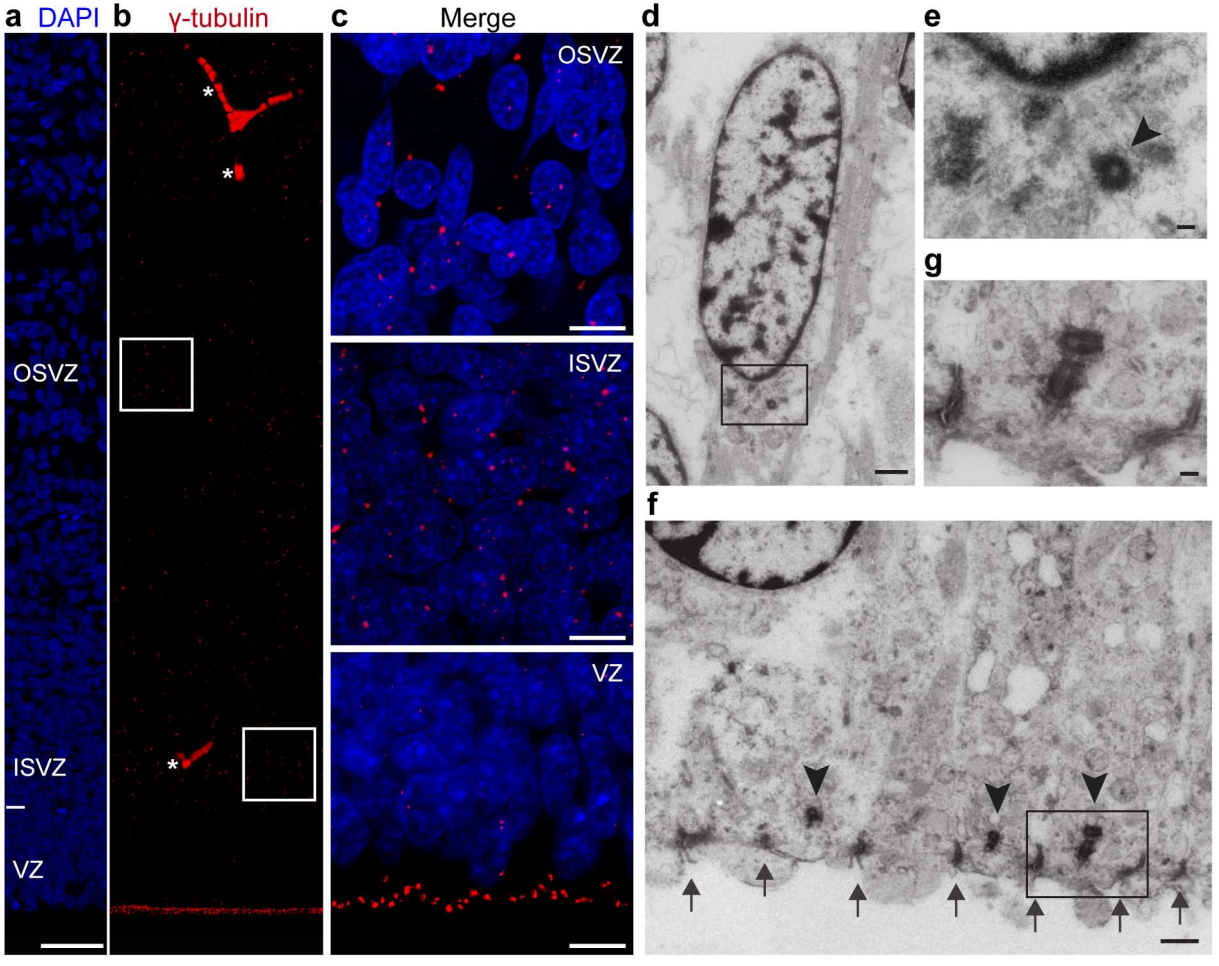

Figure-4 (Huttner)

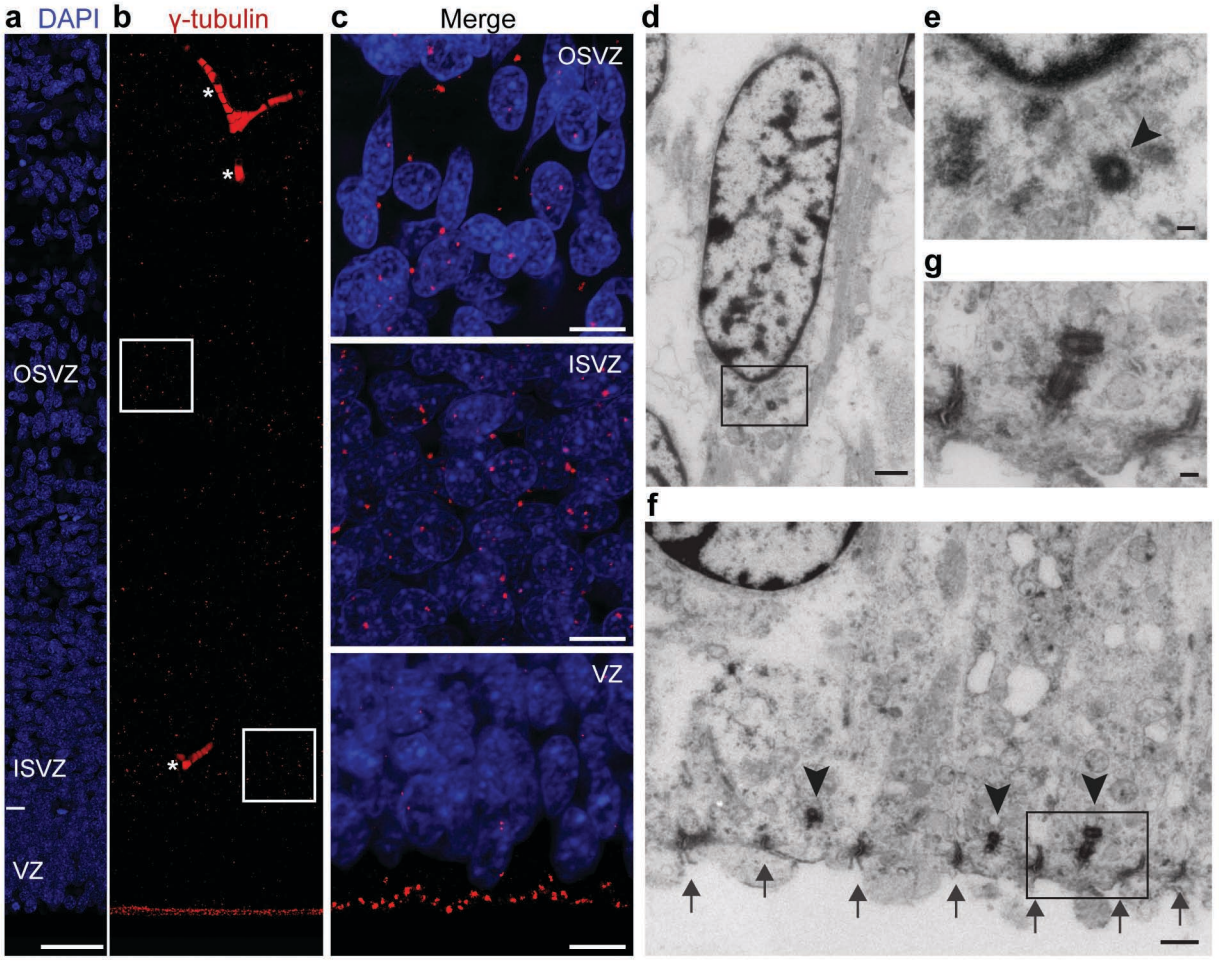

Figure-4 (Huttner)

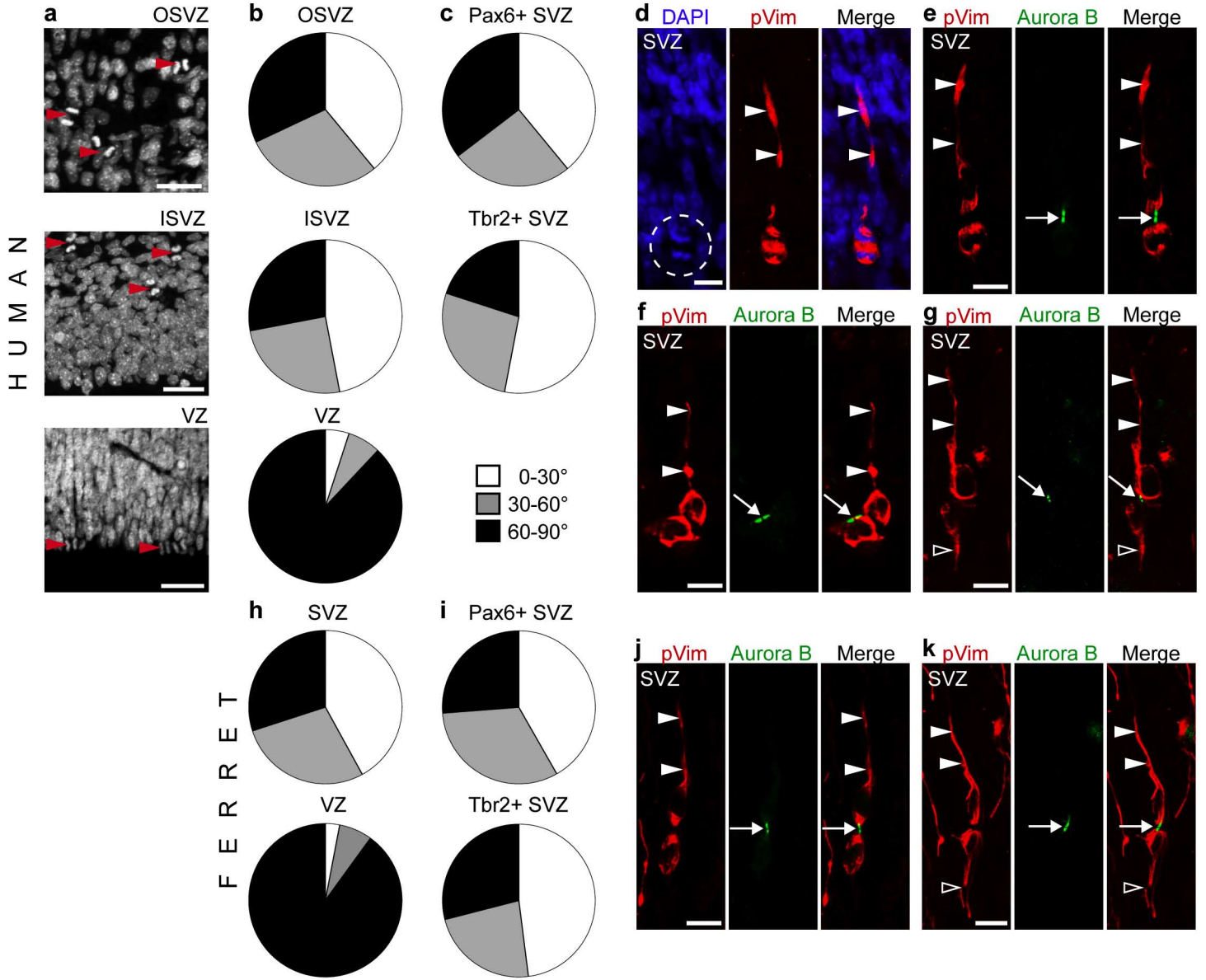

Figure-5 (Huttner)

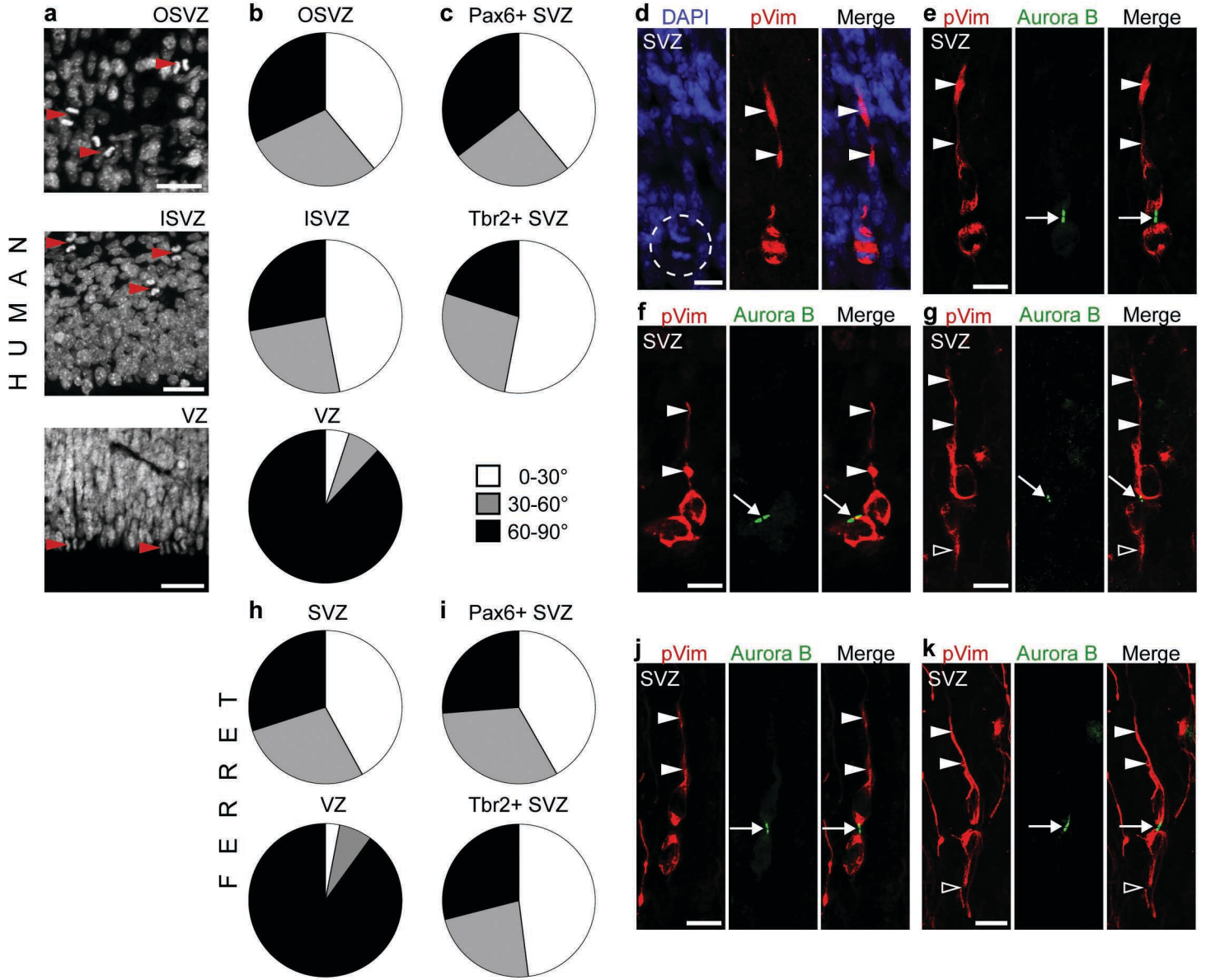

Figure-5 (Huttner)

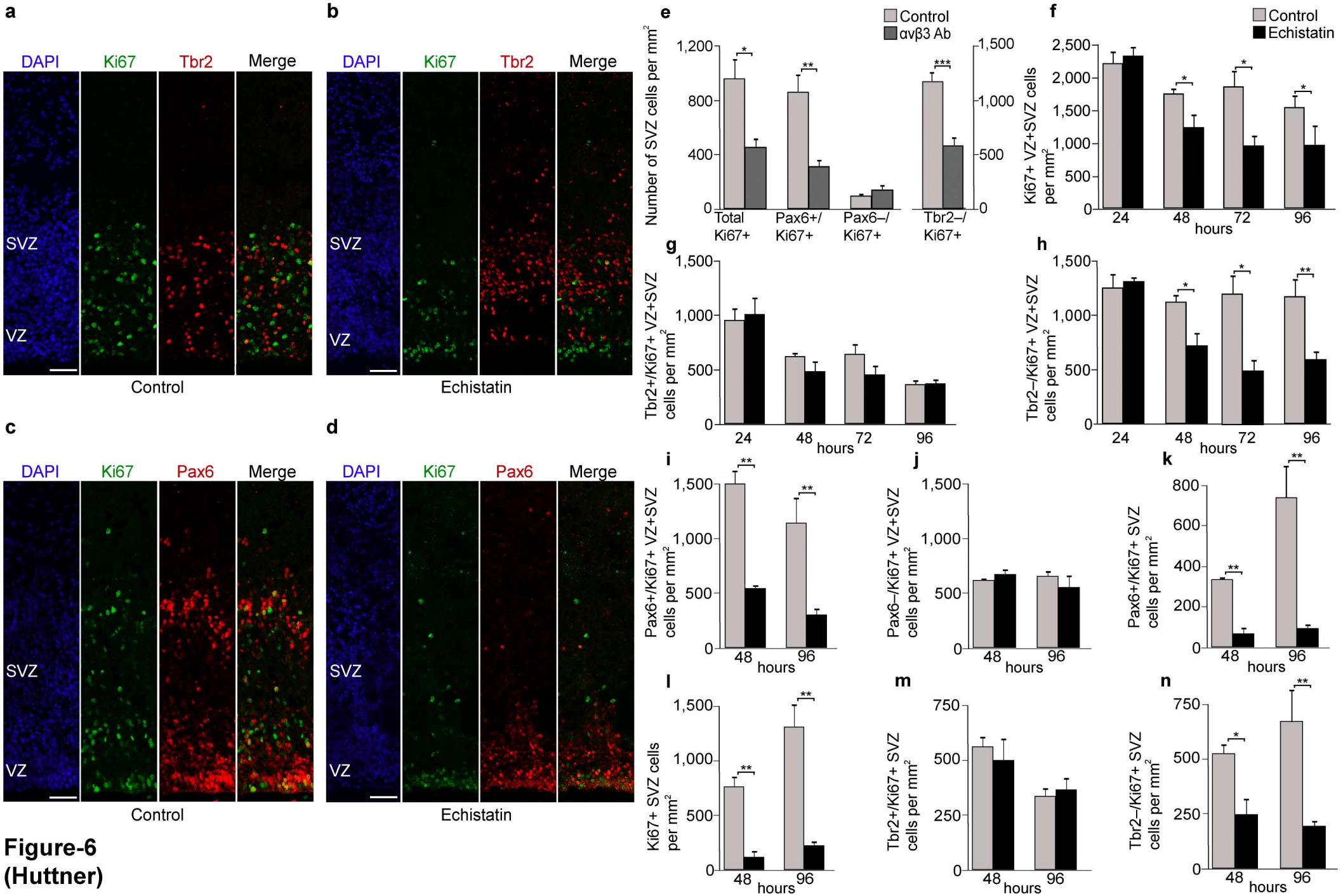

Figure-6 (Huttner)

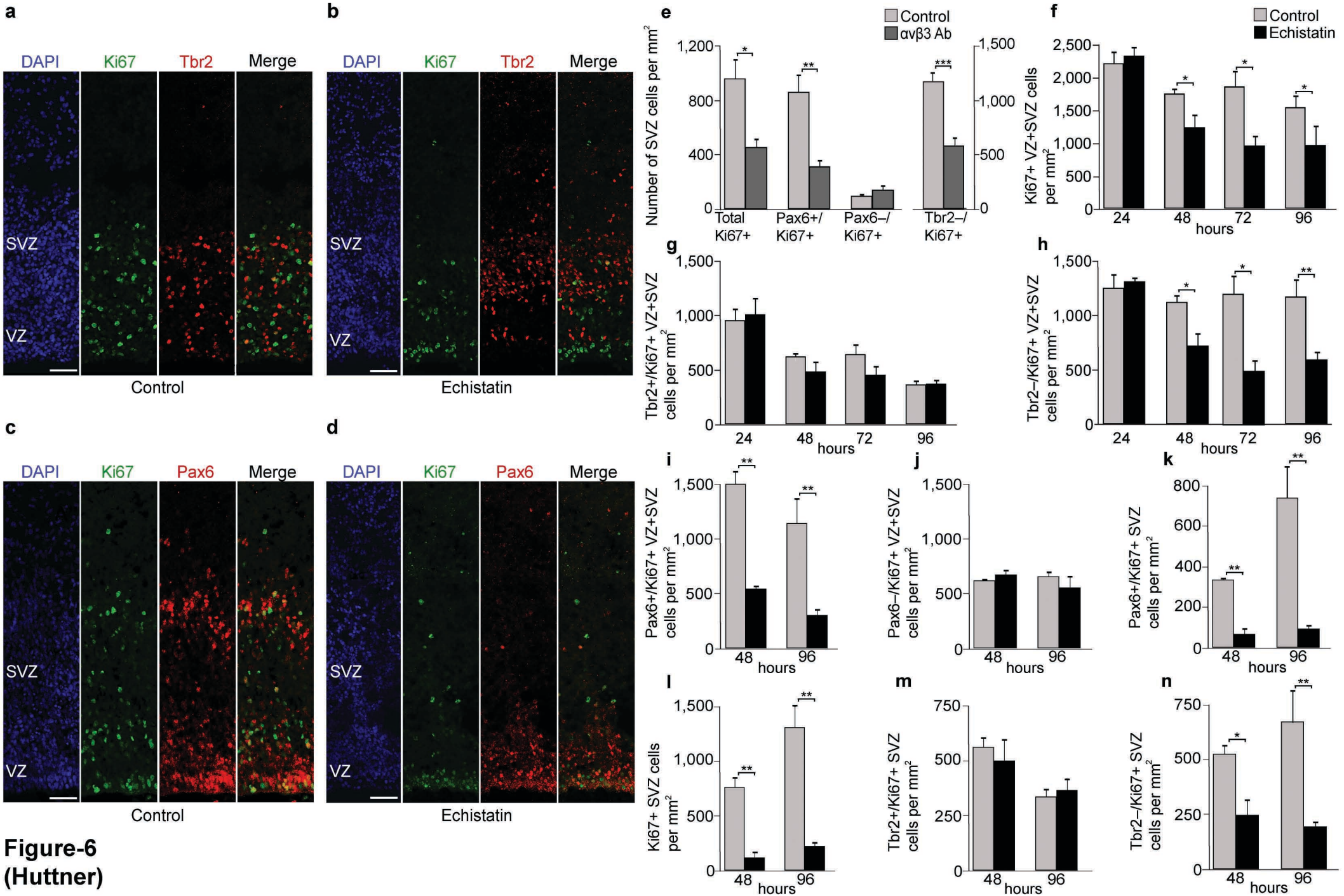

Figure-6 (Huttner)

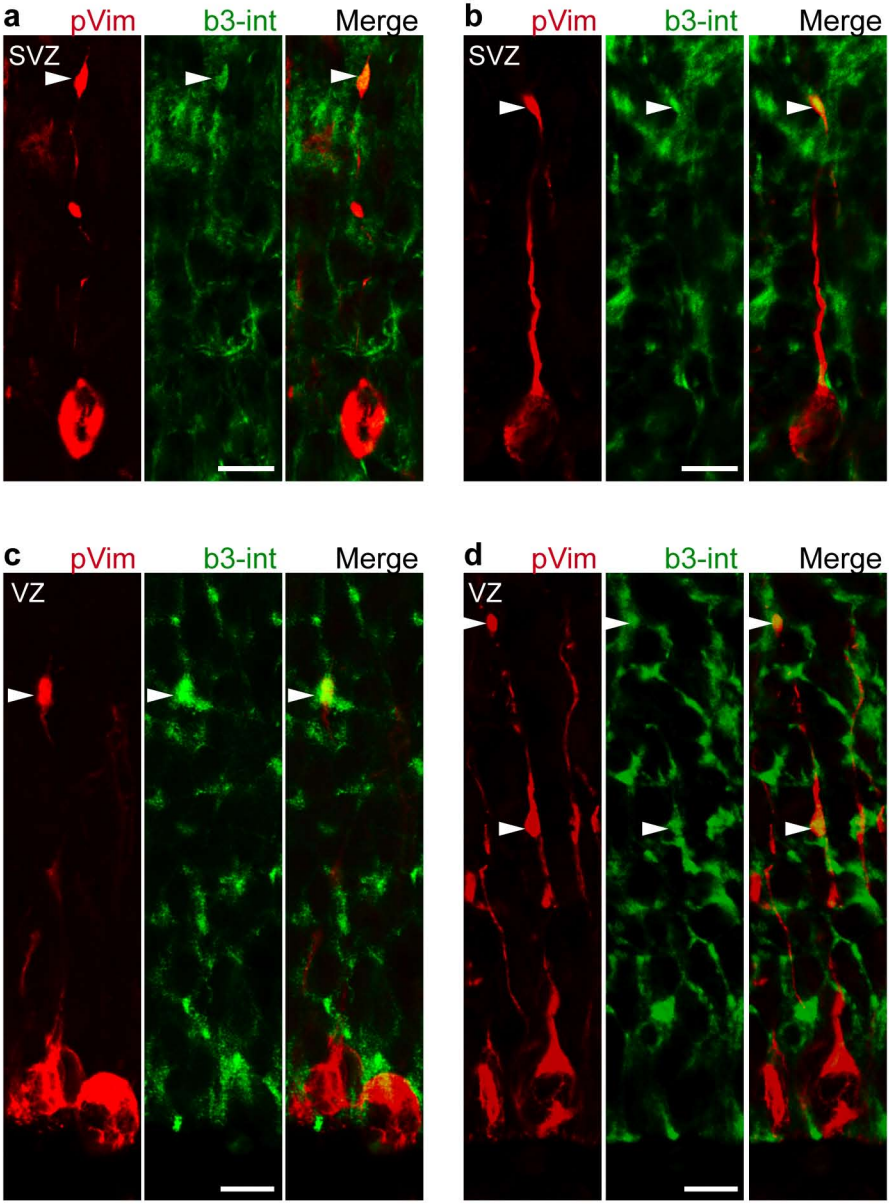

Figure-7 (Huttner)

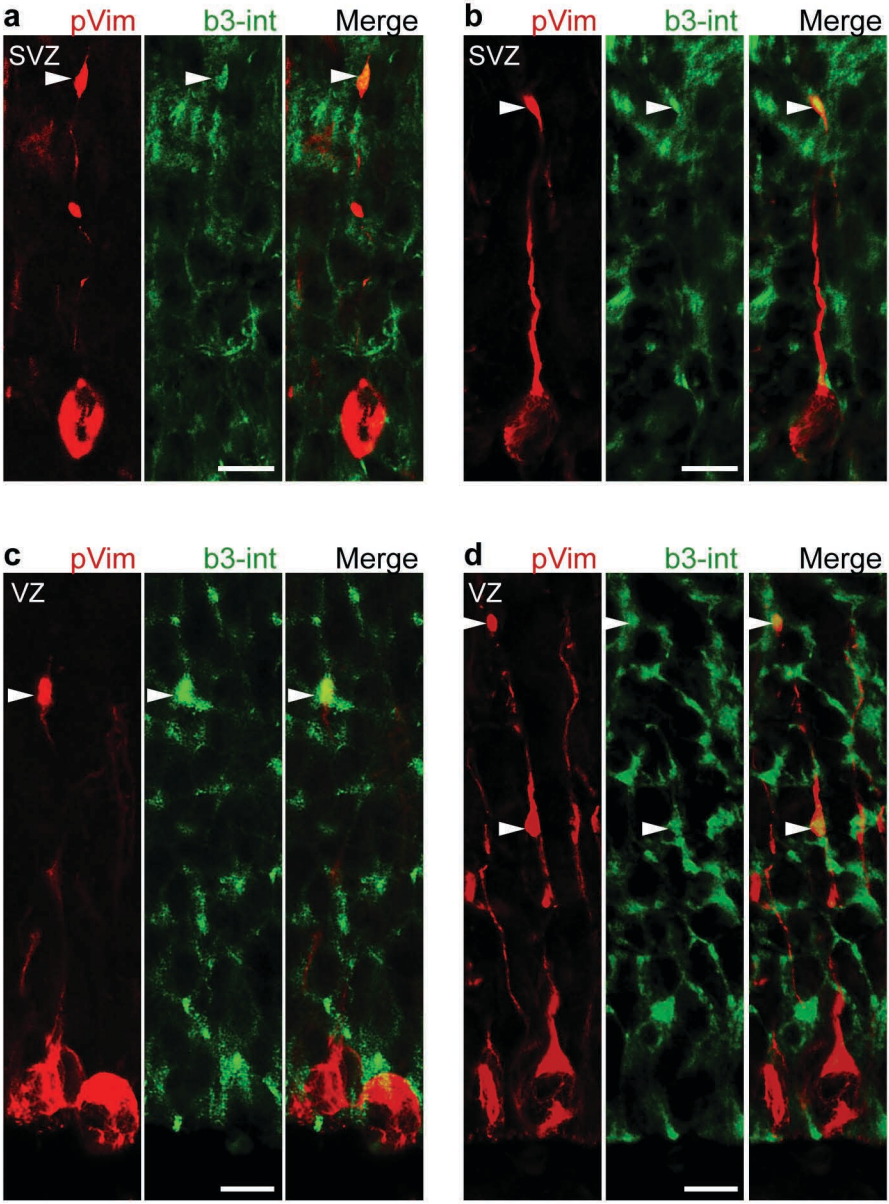

Figure-7
(Huttner)

Table 1. Occurrence of centrosomes in the human VZ and OSVZ.

	Width (μm ± SD)	No. of 200-nm sections per cell	Probability of centrosome in region per section	No. of regions analyzed	No. of centrosomes observed	Occurrence of centrosome in region per section
VZ single-cell apical region	2.52 ± 1.03	13	1 : 4.3	1419	318	1 : 4.5
OSVZ perinuclear region	6.76 ± 1.47	34	1 : 11.3	398	52	1 : 7.7

EM images of human 17-w.p.c. telencephalon were analyzed. "No. of 200-nm sections per cell" refers to the average number of 200-nm sections that would be required to cover a VZ single-cell apical region and an OSVZ perinuclear region. "Probability of centrosome in region per section" is the no. of 200-nm sections divided by three, which is the no. of 200-nm sections in which a ≥400-nm centrosome would appear. "Occurrence of centrosome in region per section" is obtained by dividing the no. of regions analyzed by the no. of centrosomes observed. For details see Methods.